M-AM-Po71 FURTHER KINETIC ANALYSIS OF THE EFFECTS OF THREE ATROPINE DERIVATIVES ON THE ENDPLATE CURRENT (EPC) OF FROG CUTANEOUS PECTORIS MUSCLE. G.G. Schofield and E.X. Albuquerque. Dept. Pharmacol. Exp. Therap., Univ. Maryland Sch. of Medicine, Baltimore, MD 21201.

Ouaternary atropine methylbromide (qATR; 30-200 μ M), homatropine (hATR; 30-100 μM), and scopolamine (SCOP; 10-100 μM), noncompetitive antagonists of the nicotinic acetylcholine receptor, decreased the peak amplitude of the endplate current (EPC) and miniature endplate current (MEPC) and altered the decay time constant (τ) of these currents. These agents induced loss of voltage sensitivity of the peak amplitude of the EPC and marked nonlinearity at hyperpolarized membrane potentials. At several membrane potentials τ is shorter in the presence of qATR, while hATR and SCOP induced a departure from a single to a double exponential decay. At -90 mV the intial decay phase of EPCs is markedly shorter than control, while the second phase is significantly longer than control. Examination of the total EPC in presence of qATR revealed a small terminal decay component which was more evident at lower concentrations (30 μM) and at depolarized potentials (-90 to -50 mV). MEPC and EPC fluctuation experiments verify the suggestion that channel behavior in the presence of hATR and SCOP is controlled by two exponential processes, whereas the channel properties in the presence of qATR are mainly controlled by a single exponential event. The data suggest that the agents alter the kinetics of channel opening in a manner similar to that of QX-222 and QX-314. The actions could be described by a sequential model involving voltage dependent rate constants controlling channel lifetime. However, new evidence also supports the idea that these agents may induce an intramolecular transformation of the ionic channel which occurs prior to channel opening. (Support: USPHS Grant NS12063 & US Army Res. Office Grant DAAG 29-78-G-0203).

M-AM-Po72 PSYCHOTOMIMETIC PHENCYCLIDINES BLOCK K CHANNELS. L.G. Aguayo[1], J.E. Warnick[1], S. Maayani[3], S.D. Glick[3], H. Weinstein[3], R.K. Ickowicz[2], M.P. Blaustein[2], and E.X. Albuquerque[1]. Dept. of Pharmacol. & Exp. Ther.[1] and Dept. of Physiol.[2], Univ. of Maryland Sch. of Med., Baltimore, MD 21201; Dept. of Pharmacol.[3], Mt. Sinai Sch. Med., City Univ. of New York, N.Y. 10029. (Intr. by Maria del Carmen Garcia G.)

Behaviorally active m-amino-PCP; 1-[1-(2-thienyl)cyclohexyl] piperidine (TCP), p-fluoro-PCP and inactive analogs [p-methoxy-PCP; p-chloro-PCP; m-NO_2-PCP; 1-piperidinocyclohexanecarbonitrile (PCC)] of PCP were examined for their interaction with the ionic channels of the nicotinic acetylcholine (ACh) receptor, excitable muscle membrane, rat brain synaptosomes and on a spatial alternation paradigm. Only PCP, m-amino PCP, TCP and p-fluoro-PCP blocked delayed rectification in frog sartorius muscles, markedly potentiated the directly elicited twitch to different extents at concentrations from 10-100 μM and significantly impaired the mean response rate in the spatial alternation paradigm. PCP and m-amino PCP blocked K-induced ^{86}Rb efflux from brain synaptosomes and increased the quantal content of endplate potentials. The inactive analogs had only small effects on these parameters at the higher concentrations (> 100 μM). All the compounds (5-100 μM) depressed peak endplate current amplitude to a similar extent (i.e., about 90%) and shortened the time constant (τ) of EPC decay in a voltage- and concentration-dependent manner. Only PCC did not affect τ_{EPC}. Cholinergic mechanisms cannot therefore explain adequately the behavioral effect of PCP and its psychoactive analogs. Since all behaviorally active components appear to block delayed rectification and/or K-induced Rb efflux and increase quantal content, it is likely that an alteration of K conductance or of calcium-activated K conductance can explain the behavioral effects of PCP. (Supported by USPHS and U.S. Army Research Office.)

M-AM-Po73 SPATIAL PROFILE OF DIVALENT ION BUFFERING IN NERVE CELL BODIES MEASURED WITH ARSENAZO III. D. Tillotson and A.L.F. Gorman (Intr. by W.C. Ullrick) Dept. of Physiology, Boston University School of Medicine, Boston MA 02118

It has been shown that the extent of buffering of injected Ca^{2+} depends upon the position of the internal injecting electrode tip; the nearer the membrane surface the smaller the measured arsenazo III absorbance signal. With use of an appropriate injecting electrode it is possible to obtain a profile of intracellular buffering by penetrating the cell in a step-wise fashion and injecting Ca^{2+} at different points inside the cell (Tillotson and Gorman, Nature, 1980, 286, 816). We used this method to obtain the spatial profiles of cellular buffering of Sr^{2+}, Mg^{2+} and Ba^{2+} (to which arsenazo III is also sensitive) in selected neurones of the marine mollusk Aplysia californica. In addition we compared the cell's ability to buffer Sr^{2+} and Ba^{2+} relative to Ca^{2+} at the same point near the cell membrane using "Theta" tubing. These latter experiments show that injected Ca^{2+} is buffered slightly more strongly than Sr^{2+} and much more strongly than Ba^{2+}. They also show that whereas the absorbance signal produced by Ca^{2+} or Sr^{2+} injection declines rapidly to the base line, the signal produced by Ba^{2+} or Mg^{2+} takes minutes to decline. The buffering profile experiments revealed the Sr^{2+} buffering to be similar to Ca^{2+}, i.e. strongest near the membrane surface. Ba^{2+} and Mg^{2+} on the other hand show a flat profile, i.e. the arsenazo signal amplitude was constant across the cell interior. An alternative interpretation of the apparent differential distribution of neuronal Ca^{2+} buffering capacity is that it results from some undefined peculiarity of the arsenazo measuring system. This interpretation is ruled out by the lack of spatial differences found with Ba^{2+} and Mg^{2+} since the differential distribution would be expected to be seen with any ion to which arsenazo III is sensitive. (Supported by NIH Grant NS 11429).

M-AM-Po74 LOCAL BIOCHEMICAL RESPONSE TO INJURY IN XENOPUS OPTIC NERVES. Szaro, B.G., and L.A. Faulkner. Dept. of Biophysics, The Johns Hopkins University, Baltimore, Maryland 21218.

Intraocularly injected, radioactive amino acids can be used to label newly synthesized proteins in retinal ganglion cells and to track their anterograde transport through the optic nerve. In order to distinguish axonally transported proteins from those labelled locally in the short (6-10 mm) optic nerve of Xenopus laevis frogs, we crushed the optic nerves at the orbit and injected S^{35} methionine into the eyes 5 min or 1 day later. At various timepoints after injecting the isotope (1,4,12, &18 hr), we compared the crushed nerves distal to the crush to normal controls using (i) TCA precipitable counts (ii) fluorographs from SDS gels run on optic nerve SDS homogenates, & (iii) autoradiography of paraffin sections. At 1 to 4 hr after injection, TCA precipitable counts from crushed nerves were greater than or comparable to normal nerves, but declined thereafter. Fluorography on SDS gels revealed 3 classes of bands: (i) bands present in normal nerves, but absent in crushed nerves,(ii) comparable bands in both nerves, and (iii) bands whose intensities had been amplified in response to the injury. Most of these amplified bands were turned over rapidly, with the exception of one predominant band of mol. wt. 46K, which persisted as long as 18 hr. Histology showed labelling of the nerve both prior to and within the crushed region. Labelling persisted in the nerve sheath several hundred microns beyond the crush, after which the crushed nerves were labelled only at background levels. Biochemistry done on segments of crushed nerves verified that the amplified bands were confined to nerve segments closest to the crush. At this time, the exact cellular origin (glial, connective tissue, circulatory, or axonal) is unclear. (We thank Y.P. Loh for advice, and NIH NS-14807 & NSF BNS-77-26987 to R.K. Hunt for support).

M-AM-Po75 HEALING AND CLONAL OUTGROWTH OF EMBRYONIC EYE-BUD GRAFTS CARRYING EXTERNALLY VISIBLE GENETIC MARKERS. Tompkins, R., Hunt, R.K., and Conway, K., Marine Biological Lab., Woods Hole, MA 02543.

We have serially followed graft healing, by camera lucida and photomicrography, in 500 Xenopus eye-buds. We excised a 'full-thickness' wedge of a host (stage 31-34, albino or wild-type) eye-bud and replaced it with a size-matched full-thickness wedge from a donor (st. 31-34, tetraploid or wild-type) bud (MS-222 1:5,000; saline of 15%HF, 5% ST as per Curr. Tops. Dev. Biol. 15, 217). The study includes wedges of different 'widths' (from narrow slivers of 10-20 cells to half-buds), orthotopic grafts at 8 sites (dorsal, D-into-D; anterodorsal, AD-into-AD etc.) and a range of heterotopic grafts (A-into-P, left A-into-right A, V-into-D, etc.). Operative failures are quick, rare and obvious (graft falls out; graft extruded from eye), even in wild-type hosts, and must be discarded. Successful grafts are trackable for 1.5 days in all strain combination (based on donor/host differences in egg pigment and basal melanin) and, after (4n and +/+) melanogenic cells blacken, as black-on-white cell patterns in albino hosts. Wedges heal, apposing graft and host cut edges, into black sectors on the otherwise white eyeball surface, widening slightly or retaining the initial width of the wedge. Individual black cells can be followed as they divide or (very rarely) die; new cells are added throughout the graft into the 3rd day post-operation, and thereafter occur only at the distal edge of the sector; cell positions are stable and become stable pattern markers. Single cell clones, laying down a long cell file in PRE, have been followed for up to 2.5 weeks of larval life. Healing is not different for hetero- vs. orthotopic grafts; so positional mismatch does not trigger intercalary growth. Recent concerns (J. Embryol. Exp. Morph. 53, 39) that our operative procedures lead to death of the graft would appear unwarranted. We thank the N.S.F. (BNS-77-26987 to R.K.H. and BNS-80-22451 to R.T.).

M-AM-Po76 REPOLARIZED RETINOTECTAL PATTERNS IN GENETICALLY MARKED EYES OF XENOPUS. Hunt, R.K., Tompkins,R., Szaro, B., and Conway, K. Marine Biological Laboratory, Woods Hole,MA 02543

Using genetic markers we have recently repeated three published experiments in which eye-bud fragments at stage 32 in Xenopus, and whole eye-buds at stage 26, were reported to show normal ('repolarized') retinotectal maps (rev. Curr. Tops. Dev. Biol. 15, 217; for operative conditions see page 237). We confirm the electrophysiologic recording data and, in individual chimerae giving complete and exquisitely normal visual projections, have determined the graft/host origins of the pigment retina (PRE) and neural retina (NR) from serial sections (Bouin's fix; 10um paraffin; Picro panceau stain). The two stage 32 bud-fragment experiments showed repolarization of the graft. In one, the dorsal half of a (pigmented) 4n right eye-bud replaced the posterior half of a (diploid) albino right eye-bud: the posterior half of the adult (normally mapping) retina was entirely pigmented in PRE and 4n in NR. In the other, an anterior wedge from the left eye of a (pigmented) 4n donor replaced an anterior wedge from the right eye of a (diploid) albino host; a 90-120° sector of anterior retina in the adult (normally mapping) eye was entirely pigmented and 4n. In the final series--Harrison's preferred paradigm that obviates de-rotation and regrowth from the wound bed--stage 26 left whole eye-buds from a (diploid) albino donor (whole = no regrowth of eye tissue in donor socket) were grafted to the right body flank of a stage 26 4n host, and 3 days later regrafted (preserving the flank orientation) into the enucleated right orbit of a stage 39 4n final carrier. The adult retina--giving a normally oriented, single continuous right-handed map (no de-rotation)--was entirely albino in PRE and diploid in NR. Regeneration of host tissue or death of the graft need not be invoked to explain repolarization of eye-bud tissue. (We thank NSF BNS-77-26987; BNS-80-22451).

M-AM-Po77 **A TWO-STAGE MODEL OF MAMMALIAN SPATIAL MEMORY.** Otto E. Rössler, Institute for Physical and Theoretical Chemistry, U. of Tübingen, 7400 Tübingen, W. Germany

The hippocampus, the most regularly wired structure of the mammalian cortex, receives increasing attention (O'Keefe, J. and L. Nadel, The Hippocampus as a Cognitive Map, Oxford U.P., 1978; Molecular, Cellular and Behavioral Neurobiology of the Hippocampus, W. Seifert, ed., Academic, 1982). This organ appears indispensable for both short-term and long-term spatial orientation, if the environment and/or the spatio-temporal task is sufficiently complicated. However, short-term tasks can be performed in its absence if there is no distraction (and 'very long-term' spatial memory is unimpaired). The following model takes account of all major observations. a) There is a universal spatio-temporal simulator of reverberatory type (which hence is not a 'memory' in the strict sense) acting as a short-term memory in the absence of distraction; see Rössler, BioSystems 13:203, 1981, for a functional block diagram. b) There is as a first stage a 'back up memory' that can be loaded back into the simulator after distraction (interrupted reverberation). It also sends its content ('frames') into (c) and retrieves them from there. c) There is a content-addressable 'long-term memory' accessible to (b). Specifically, (b) is thought to be implemented by the hippocampus. In (b), there is both exogenous environmental information and (endogenous) 'force field' information attached to it (Rössler, Progr. Theor. Biol. 6:147, 1981). These specific potentials, if reactivated exogenously after a distraction, act as 'haul-in lines' for resuspending information from (b) into (a). Moreover, their both environment- and state-dependent combinations are unique enough to be used as a scalar 'color code' for storing away the whole content of (b) into (c) and retrieving it back - in the way of a typical content addressable memory (CAM) of parallel type. With increasing familiarity, less and less 'color bits' (and less and less hippocampus) suffice for retrieval.

M-AM-Po78 TERBIUM FLUORESCENCE MICROSPECTROPHOTOMETRY OF CULTURED NEURONS. Robert G. Canada. Laboratory of Neurophyisology. National Institute of Neurological and Communicative Disorders and Stroke, Bethesda, Maryland 20205.

An ultraviolet microspectrofluorometer was constructed to measure the fluorescence characteristics of Tb^{3+} bound to cultured mouse spinal cord (SC) and dorsal root ganglion (DRG) neurons. The binding of Tb^{3+} to cultured neurons resulted in the enhancement of its fluorescence emission intensity. Inspection of the Tb^{3+} excitation spectra revealed that the fluorescence enhancement was sensitized by nonradiative resonant energy transfer from nearby aromatic residues. The fluorescence intensity of the Tb^{3+}-neuron complex was dependent on the type of neuron under question, in that, under similar conditions, the Tb^{3+}-DRG complex displayed a greater relative fluorescence intensity than the Tb^{3+}-SC complex. Likewise, the visual fluorescent appearance of a cell was dependent on its neuronal type. The cell bodies of DRG neurons were completely covered in a dense fluorescent blanket. The fluorescence from the SC cell bodies appeared in a discontinuous pattern. Background cells did not display appreciable amounts of Tb^{3+} fluorescence. The fluorescence intensity of the Tb^{3+}-neuron complex was dramatically reduced in the presence of a high concentration of Ca^{2+}. The fluorescence properties of the Tb^{3+}-neuron complex were in close agreement with those obtained from our solution studies using synaptic membranes, synaptosomes and dissociated spinal cord cells in suspension. It is suggested that Tb^{3+} binds to Ca^{2+}-binding sites on the surface membrane of neurons.

M-AM-Po79 OPTICAL MEASUREMENT OF POTENTIAL CHANGES IN AXONS AND PROCESSES OF NEURONS OF A BARNACLE GANGLION. W.N. Ross and V. Krauthamer*, Dept. of Physiology, N.Y. Medical College, Valhalla, N.Y.

Optical recordings of transmembrane voltages at multiple sites on single cells, combined with standard intracellular recording and staining methods, allows for an analysis of the regional properties of neurons. We have used this combination of techniques to examine cells of the supraesophageal ganglion of the giant barnacle, Balanus nubilus.

Ganglia were stained with the voltage-sensitive dye, NK2367. The preparation was mounted on the stage of a Zeiss Universal Microscope and imaged with a x40 water-immersion lens onto a 32 element array of photodiodes, each element corresponding to 40 x 40 um^2 in the object plane. Large cells along the anteromedial margin were impaled with a microelectrode and action potentials and hyperpolarizing responses were evoked alternatively and repetitively. The resulting changes in absorption, detected on each element at 720 ± 25 nm, were averaged on a laboratory computer. Opticaly detected signals could be seen from cell bodies, axons, and processes. Measurements of the time-to-peak, width, and amplitude of the optically detected action potentials established that the spike propogated actively along the axon and passively into the neuropilar processes of these cells. Similarly, when square hyperpolarizing pulses were injected into the soma, optical signals corresponding to the electrotonic spread of these pulses were detected in axons and processes. These optical records were compared with those predicted from a passive membrane model based on cellular geometry determined from Lucifer Yellow dye injections and electrical measurements made with the intracellular electrode.

Supported by UPHS grant NS16295, fellowship NS06929, and the I.T. Hirschl Foundation.

M-AM-Po80 A METHOD FOR OVERCOMING NON-ISOPOTENTIALITY IN A PASSIVE MONOPOLAR NEURON. Claudio I. Valenzuela. Neural and Behavioral Biology Program, University of Illinois, Urbana, IL.

Neuroscientists commonly lack isopotential conditions while conducting intracellular stimulation and recording experiments. The present work developed a method for overcoming non-isopotentiality in a linear (passive) model of an intact monopolar neuron with an approximately spherical soma and an approximately cylindrical dendrite or axon (or equivalent cable) of length greater than or equal to 3 space-constants. The identification of the currents that flow into each of the neuron parts (e.g., soma, axon, etc.) was achieved by means of the deconvolution of the estimated impulse-response functions of the neuron parts and the voltage recorded at the soma of the neuron.

One of the key theoretical manipulations of the identification method proposed here is the instantaneous voltage-clamping of the soma to resting potential ("quasi-short-circuiting"). When the neuron voltage prior to clamping is the steady-state voltage caused by step current injection at the soma quasi-short-circuiting provides a clamping current with a time-derivative (except at zero):

$$\frac{d}{dt} I_{clamp}(t) = (2 V_0/\sqrt{\pi} R_{ICD}) \text{ EXP}(-t/\tau_m) \quad (1)$$

which can be used to estimate the parameters R_{ICD} (dendrite input resistance as seen from the soma) and τ_m (passive membrane time-constant). V_0 is the soma voltage prior to voltage-clamping. R_{ICD} and τ_m were instrumental in the identification of the impulse-response functions of the neuron parts. The rapidity with which the derivative of the clamping current may converge to equation 1 above when the voltage clamper used is non-instantaneous but fast is currently under investigation.

Supported by a Consejo Mexicano de Ciencia y Tecnologia (CONACYT) Scholarship.

M-AM-Po81 IMPROVED FLUORESCENT PROBES FOR THE MEASUREMENT OF RAPID CHANGES IN MEMBRANE POTENTIAL. A. Grinvald, R. Hildesheim, L.B. Cohen, and B.M. Salzberg. The Weizmann Institute of Science, Yale University, and the University of Pennsylvania.

In order to improve the quality of fluorescent potentiometric probes, and to permit their use for recording from neuronal arborizations, twenty new styryl dyes were synthesized and several of these were tested on squid giant axons, leech segmental ganglia, neuroblastoma cells maintained in monolayer cultures, avian embryonic heart muscle, and liposomes. Some of these new probes are significantly better than any reported previously. The optical measurements were made with a standard fluorescence microscope equipped with a DC mercury illuminator. Using the triene styryl RH-237 or the diene, RH-160, a signal-to-noise ratio of 40:1 was obtained in optical recording of action potentials from neuroblastoma cells in culture. The fractional changes in fluorescence were as large as 14% / 100 mV. Photodynamic damage and bleaching were three to five times less significant with the new probes compared to WW 781 or WW 802.

The dye RH-160 (a Zwitterionic dye) gave large signals when tested as an intracellular probe by perfusion in a voltage clamped squid giant axon preparation. The fluorescent dyes RH-376 and RH-292 have negative and doubly positive charges, respectively; they could be injected iontophoretically into neurons, and they spread well throughout their processes. Thus, it seems likely that the study of the integrative properties of the dendritic and axonal arborizations of single cells in intact tissues will be facilitated by such fluorescence measurements.

Supported by PHS grants NS 16824, NS 14716, NS 08437, and a grant from the US-Israel Binational Science Foundation.

M-AM-Po82 A BUFFERING MODEL FOR CALCIUM DEPENDENT NEUROTRANSMITTER RELEASE. D.A. Nachshen and P. Drapeau. (Intro. by T. Tiffert) Department of Physiology, University of Maryland, School of Medicine, Baltimore, Md. 21201.

A simple model is proposed, whereby a single buffering system for intracellular calcium accounts for the steep external Ca- dependence of neurotransmitter release during depolarization of the presynaptic nerve terminal. We assume 1) that Ca entry is instantaneous and saturable, 2) that part of the Ca load is immediately sequestered by a saturable buffer, and 3) that transmitter release is proportional to the free intraterminal Ca concentration, Ca_i. Solving for Ca_i as a function of external Ca gives a simple expression that depends only on the half-saturation constants and maximal rates of activity of the Ca entry and buffering mechanisms. The novel feature of this model is that it explains the apparent cooperative relationship between transmitter release and extracellular Ca, without invoking cooperative Ca binding. Supported by NIH grant NS-16461 to D.A.N., and M.R.C of Canada Fellowship to P.D.

M-AM-Po83 QUANTITATIVE DESCRIPTION OF STIMULATION-INDUCED CHANGES IN TRANSMITTER RELEASE AT THE FROG NEUROMUSCULAR JUNCTION. Karl L. Magleby and Janet E. Zengel, Dept. of Physiology and Biophysics, University of Miami School of Medicine, Miami FL 33101, and Depts. of Neuroscience and Neurosurgery, University of Florida College of Medicine, Gainesville, FL 32610.

Endplate potentials were recorded from frog sartorius neuromuscular junctions under conditions of greatly reduced quantal contents to develop a quantitative working hypothesis for stimulation-induced changes in transmitter release. Four general models relating potentiation, augmentation, and the first and second components of facilitation to transmitter release were developed. These general models were then tested by incorporating into them equations for the kinetic properties of the four components of increased transmitter release and examining the ability of the resulting sets of simultaneous equations to predict transmitter release. Three of the models were essentially consistent with the observation that augmentation had a multiplicative type relationship to facilitation. These models could also predict the effect of frequency and duration of repetitive stimulation on endplate potential amplitude during and after prolonged (40 sec) trains including the response to step changes in stimulation rate. These models extend by about two orders of magnitude the duration of stimulation-induced changes in transmitter release that can be accounted for, and these results show that the combined kinetic properties of potentiation, augmentation, and the two components of facilitation are sufficient to account for stimulation-induced changes in transmitter release under conditions of low quantal content. Supported by NIH grant NS 10277.

M-AM-Po84 ANESTHETIC GASES RETARD ELECTRON MOBILITY. RC Watt, SR Hameroff, JD Borel, Department of Anesthesiology, University of Arizona, Tucson, AZ 85724

Anesthetic gas molecules inhibit excited state luminescence in bacterial and firefly enzyme systems, and excited electron states in intraprotein hydrophobic regions have been implicated in protein conformational regulation. To investigate anesthetic mechanisms, we've studied direct anesthetic effects on gaseous phase electron mobility.

An E-field generator delivers a 20 KV/cm field to a chamber through which gas flows (biological transmembrane field:100 KV/cm). Gaseous electron excitation results in visible corona discharge and 100-400 μA current spikes which, after filtering of generator waveform, were counted. Random sequences of 6 gases in oxygen (5 liters/min) flowed through the excitation chamber. Gas samples taken proximal to the chamber were analyzed by gas chromatography for halothane, enflurane, and isoflurane and by oxygen polarimetry for nitrous oxide, nitrogen, and helium.

Potent anesthetics (halothane, enflurane, isoflurane) strongly inhibited excitation. Nitrous oxide, a weaker anesthetic, inhibited less strongly. Nitrogen in oxygen had minimal effects and helium increased excitation. Corona discharge was also observed to correlate with current spike counts and anesthetic effect.

Current spikes represent electrons accelerated by the applied field. Anesthetic inhibition of gaseous ionization, electron mobility and excitation could occur by Van der Waal's dipole interactions altering dielectric, "mean free path," or excited state quenching and be similar to anesthetic effects in enzyme bioluminescence and perhaps true sites of anesthetic action. Retardation of electron mobility in intraprotein hydrophobic regions could inhibit ion channel, receptor, or cytoskeletal function and result in "anesthesia."

M-AM-Po85 Rho, J.H. and Hunt, R.K. TOPOLOGICAL MAPPING OF RETINAL GANGLION CELLS ACROSS SURGICALLY RESTRUCTURED OPTIC TECTA IN XENOPUS; Jenkins Department of Biophysics, Johns Hopkins University, Baltimore, Md. 21218

Electrophysiology has proved to be an effective method of localizing the distribution of the axonal arborizations of retinal ganglion cells across the surface of the optic tectum. When the surface is altered, by the implantation of tissue grafts from different regions of tectum, the regenerated visual projections are disrupted in the region of the implant. Implants from different regions affect the regenerated pattern differentially; ie. rotated grafts induce retinal ganglion fibers to map backwards, etc. We find that other defects, including duplicate points, scotomas, and other topological disruptions occur in or extend into tectal regions away from the implant. Abrupt discontinuities can be seen in the topography of tectal regions that were not involved in the surgery. For example, when a central region of medial tectum was replaced by a heterotopic graft taken from the lateral edge of the contralateral lobe (Rho and Hunt, Dev. Biol. 80, 436-453), the optic fibers mapped differently in three regions of the tectum. The central region was more disordered and its topography differed radically from the surrounding map. The surrounding map, while grossly 'normal' relative to the central region, was actually broken by a discontinuity into two distinct subregions. Each subregion has a different near-normal topography -- distinct from one another and from the pattern seen in unoperated frogs. We suggest these distant perturbations may have been caused by healing forces other than positional affinities of optic fibers for tectal cells. (Supported by NIH NS 14807 and NSF BNS 77 26987 to R.K. Hunt)

M-AM-Po86 DIVALENT CATIONS DIFFERENTIALLY SUPPORT TRANSMISSION AT THE SQUID GIANT SYNAPSE. George Augustine and Roger Eckert. Department of Biology, and Ahmanson Laboratory of Neurobiology, UCLA, Los Angeles, CA, and Marine Biological Laboratory, Woods Hole, Mass.

The divalent cations Sr and Ba support secretion in a variety of cells. We have examined the ability of these ions to support transmission at the squid giant synapse, where it is possible to concurrently measure pre- and postsynaptic potentials and currents. Experiments were performed on the most distal giant synapse of Loligo pealei. Initially the postsynaptic axon was voltage clamped, using the postsynaptic current (PSC) as a measure of transmitter release. Substitution of Sr or Ba for Ca decreased the PSC. In Sr PSC amplitude was reduced to 12 ± 3% (S.E.M., n=5) and in Ba 0.5 ± 0.1% (n=5), compared to Ca. Presynaptic action potential amplitude was unchanged in Sr or Ba and duration was unchanged in Sr and greater (30 ± 12%, n=5) in Ba. Thus the effects of Sr and Ba were not due to reductions in the presynaptic action potential. Presynaptic currents carried by Ca, Sr and Ba were measured using 2- or 3-electrode voltage clamp methods. The amplitude of currents elicited by brief depolarizing pulses was similar in all three cations, although the resultant postsynaptic potentials (PSPs) were not. Transfer curves relating presynaptic current to PSP amplitude indicated that at all presynaptic current intensities, PSPs were largest in Ca and smallest in Ba. In summary, divalent cations support transmission at the squid giant synapse, in the sequence Ca > Sr >> Ba. Their differential ability to support transmission is not due to their presynaptic permeability or to their effects on presynaptic action potentials. Supported by MDA Postdoctoral Fellowship and USPHS 5-S07 RR07009-16.

M-AM-Po87 INTERACTION OF CALCIUM IONS AND BARBITURATES ON THE FIRING ACTIVITY OF A SINGLE NEURON. K.-S. Tan and S.H. Roth, Department of Pharmacology & Therapeutics, University of Calgary, Calgary, Alberta. Canada. T2N 1N4.

The effects of three barbiturates (methohexital, pentobarbital and phenobarbital) have been examined on the firing activity of a single isolated neuron - the stretch receptor of the crayfish. Methohexital and pentobarbital depress the firing frequency in a concentration-dependent manner and produce opposite effects with that of phenobarbital. At higher concentrations (>0.7mM), methohexital produces a characteristic rhythmical burst pattern with an intraburst frequency of ∿60-70 Hz. This is not observed with pentobarbital, the pattern remains rhythmical. In contrast, phenobarbital produces a concentration-dependent excitation in firing activity, and at higher concentrations (>1mM) alters the firing pattern. Bursting activity with intraburst frequency of 10-15 Hz is observed. During washout of either methohexital or pentobarbital, firing frequency is initially enhanced, followed with an exponential decay to control levels. Washout of phenobarbital produces a depression, followed with complete recovery. Variation of Ca^{++} ions in the bathing medium can also change the firing activity. High Ca^{++} produces a depressant effect similar to that of pentobarbital, and low Ca^{++} produces excitation similar to phenobarbital. Excess Ca^{++} can antagonize the enhancement effect produced by phenobarbital and low Ca^{++} antagonizes the depressant effects of pentobarbital and methohexital. The results suggest barbiturates may modify Ca^{++} ion transmembrane activity involved during the firing cycle, and different barbiturates can produce different effects on Ca^{++} activity.

SUPPORTED by the Alberta Heritage Foundation for Medical Research and the Canadian MRC.

M-AM-Po88 SERIES RESISTANCE MEASURED BY INTEGRALS OF TRANSIENTS. R.S. Eisenberg, R.T. Mathias, and J.L. Rae. Dept. of Physiology, Rush Medical College. 1750 W. Harrison, Chicago, IL 60612.

Voltage clamp systems must compensate for potential drops across resistance R_s in series with the membrane if the voltage across the membrane is to be a faithful replica of the command voltage, independent of membrane current. The value of R_s must be accurately known; yet the usual measurements made from the time domain response to step currents or voltages are subject to substantial error. The series resistance is related to the derivatives of the frequency domain admittance Y_k evaluated at s=0, namely $R_s = 1/(Y_0 - 2Y_1^2/Y_2)$. If the input signal is a step of voltage $v(\infty)$ giving final current $i(\infty)$, these frequency domain derivatives can be conveniently and accurately measured by integrating the current response i(t) in the time domain, as follows:

$$Y_{k+1} = \frac{k+1}{v(\infty)} \int_0^T (-t)^k \{i(t)-i(\infty)\}dt \quad \text{for} \quad k=0,1,2\ldots; \quad \text{with } Y_0=i(\infty)/v(\infty)$$

The integration time T must be the smallest time at which the integrand is negligible. Voltage inputs other than steps can be analyzed by related formulae, involving additional analagous integrals of v(t). Simulations show that this approach provides a convenient accurate estimate of R_s even in the presence of large amounts of noise, even if the input signal is dramatically over or underdamped. The above formulae assume an ideal lumped membrane resistance, membrane capacitance, and series resistance, but they can be generalized when more accurate and complex representations of the membrane and series impedance are determined.

M-AM-Po89 Ca ENTRY AT REST AND DURING PROLONGED DEPOLARIZATION IN DIALYZED SQUID AXONS.
Rojas, H., DiPolo, R. and Beaugé*, L. C.B.B., IVIC, Apartado 1827, Caracas 1010A, Venezuela.
*Instituto M. y M. Ferreyra, Córdoba, Argentina.

Ca influx has been studied in squid axons under internal dialysis control. In axons dialyzed with "normal" physiological conditions (Na_i = 40-50 mM, Ca_i^{2+} = 0.06-0.1 μM, ATP = 2 mM, K_i =310 mM), 70% of the resting Ca influx is sensitive to external TTX ($K_{0.5} \simeq 5$ nM), 20% of it can be accounted by the reversal of the Na-Ca exchange, and the remaining fraction (10%) is insensitive to TTX, D-600, and Na_i. The Ca antagonic drug D-600 (50-100 μM) has an inhibitory effect on the resting Ca influx. This compound was found to affect both the TTX sensitive and the Na_i-dependent Ca influx components. In the presence of Na_i and ATP, Ca_i^{2+} activates the carrier mediated Ca entry (Na_i-dependent Ca influx). Most of the activation occurs in the submicromolar range of Ca_i^{2+} concentrations ($K_{0.5} \simeq 0.6$ μM). In the absence of Na_i and/or ATP, no activation of Ca influx by Ca_i^{2+} was found up to about 5 μM Ca_i^{2+}. Prolonged depolarization with high K_o causes an increase in Ca influx sustained for long time (minutes). Depolarizing the axons by removing K_i causes the same effect. This depolarization-induced Ca entry was only observed in axons containing Na_i. In the absence of Na_i, Ca influx decreases with increasing K_o. The activation of the carrier mediated Ca entry (electrogenic Na/Ca exchange) by membrane depolarization was found to be markedly dependent on the $|Ca^{2+}|_i$. Increasing the $|Ca^{2+}|_i$ from 0.1 to 0.6 μM causes a ten fold increase in the extra Ca influx induced by a K-depolarization.

M-AM-Po90 PRESYNAPTIC EFFECT OF FRACTIONS ISOLATED FROM THE SPONGE Tedania ignis. C.Sevcik and C.A. Barboza. Laboratory of Cellular Neuropharmacology, Centro de Biofísica y Bioquímica, Instituto Venezolano de Investigaciónes Científicas (IVIC), Apartado 1827, Caracas 1010A, Venezuela. The isolation of two fraction with presynaptic effect from sponge Tedania ignis has been achieved. The crude preparation obtained by ethanolic extraction (1:1w/v), concentration under reduced pressure to 10% of the extract volume, and precipitation with acetone, kills mice by i.p. injection. The death of the mice occurs by generalized flaccid paralysis. Treatment of the extract with glacial Acetic Acid (1:1v/v) or concentrated amonia (1:1 v/v) produces abundant precipitate but the biological activity remains in the supernatant. Elution through AG-50X8 cation exchange resin inactivates the extract and the biological activity cannot be recovered from the column even by elution with 2M Acetic Acid or 1M ammonia. In neuromuscular junctions of Rana pipiens, the crude fraction decreases the amplitude of the evoqued endplate potential and increases the frequency of miniature endplate potentials without effects on their amplitude or shape. Elution with 1M Acetic Acid through Sepadex G15 produces three peaks within column volume but only one of them contains the biological activity, the compounds in this peak posses a molecular weight close to 1000 daltons. Elution with 1M Acetic Acid through Bio Gel P2 produces 9 peaks, but only 2 of them are biologicaly active. One of these fractions (fα)increases the frequency of miniatures,and another fraction (fβ) inhibits the evoqued release of neurotransmitter. None of the fractions change the amplitude or shape of miniature endplate potentials, nor do they modify the resting membrane or action potentials in frog muscle or squid giant axons. The effect of fβ may be antagonized by raising the extra cellular Ca concentration.

M-AM-Po91 CHEMICALLY-GATED CATION CHANNELS FROM OLFACTORY EPITHELIAL HOMOGENATES. Vitaly Vodyanoy and Randall B. Murphy, Department of Chemistry, and Laboratory of Radiation and Solid State Physics, New York University, 4 Washington Place, New York, NY 10003.

Rat olfactory epithelial homogenates incubated on one side of a planar phosphatidylcholin bimolecular membrane induced fluctuations and a sharp increase in the conductance when the concentration of diethyl sulfide (odorant in the rat) delivered into the same side of the membrane reached the threshold of 0.1÷0.2 nM in 20mM KCl, 20 mM NaCl, 2 mM $CaCl_2$, pH 7.4. An essentially solvent-free membrane of area ∿2 mm^2 has been prepared by passing a hydrostatically closed chamber successively through a single monolayer interface. A linear correlation between relative conductance evoked by diethyl sulfide and the logarithm of its concentration over three orders of magnitude (10^{-11}- 10^{-8}M) has been observed. The response to diethyl sulfide could be completely deactivated by the K^+-channel blocker 4-aminopyridine (0.125 mM). Analysis of spontaneously fluctuating single channel indicated a conductance of (6±1)x10^{-11}mho (in above solution). This corresponds to a mean channel open time of 29.3±7.8 (S.E.) sec. In the presence of diethyl sulfide the mean channel open time was increased, and significant deviation from random channel opening in time was observed. Using a Langmuir isotherm the number of excited channels could be estimated as a function of the diethyl sulfide concentration, assuming independent behavior of channels. A study of the voltage-current characteristics of the channels indicated a lack of effect of electric field upon the probability of an open channel state within 0÷100 mV. (Supported by grant DA0009 from NBS).

M-AM-Po92 Mechanical Excitability of Epithelial cells in culture. G. Roy and R. Sauvé, Dept. de physique, Université de Montréal, P. Québec, Can.

A well known human cancer cell line in culture, Hela, have shown an electrical response when a mechanical shock is given to them. Upon penetration with a microelectrode, the recorded potential is large (-53 mV average) and decreases to a lower stable level of -37 mV after about one minute. If a mechanical shock is given to the recording table, a hyperpolarization of varying amplitude lasting about 20-30 seconds is observed. Also a large positive or negative current pulse (30 n amp) can evoke the same response. Such currents could provoque a mechanical vibration of the electrode tip because of heating. This hyperpolarization is caused by a change in the K^+ permeability of the membrane. The resistance is measured and found to be lower at the peak potential. The stable potential value is in accordance with the measured Cl^-ratio. The value of the resistance at the stable level is related to the Cl^-permeability. In order to explain the hyperpolarizing response, a large increase of P_k/P_{cl} is required. External Ca^{++} is not required to produce the response, but a liberation of Ca^{++} from internal compartments could be the trigger of this K^+ current. Injection of Ca^{++} through the microelectrode produces similar responses. Also replacing external Na^+ by K^+ produces a large increase of P_k/P_{cl}. If an opening of K^+ pores is responsible for these currents, they have very asymetric characteristics being opened by Ca^{++} inside and by the removal of Na^+ outside. Current-voltage curves also demonstrate a characteristic typical of anomalous rectification.

Supported by a grant of the Natural Science and Engineering Research Council of Canada

M-AM-Po93 EFFECT OF MB^+ ON SODIUM AND GATING CURRENTS IN CRAYFISH GIANT AXON. Starkus, J.G., M.D. Rayner, and S.T. Heggeness. Dept. of Physiology, Univ. of Hawaii, Honolulu, HI 96822.

In perfused axons, internal application of the cationic dye Methylene Blue (MB^+ binds strongly to carboxyl groups at conc. of 1 mM) produces a fully and rapidly reversible acceleration in Na kinetics, decreasing the time to peak as well as the peak sodium current. Potassium currents were totally blocked by internal perfusion with 1 mM 4AP and 20 mM TEA.

Signal averaging and exponential curve stripping (Rayner and Starkus*) of Na and gating currents reveals at least 6 ionic components and 4 gating components. Multiple components on the falling phase of the Na current are described as Tau 1 thru 4 and on the rising phase as Tau 5 and 6. The fastest gating components are identified as Tau F_1 and F_2 and the slowest as Tau S_1 and S_2. MB^+ reversibly suppresses the slowest components in both I_{Na} (Tau 1) and gating (Tau S_1), and accelerates the ionic components (Tau 2,3 and 4) by a factor of three and Tau 5 by a factor of two. All 4 components of gating currents are smaller in size after MB^+ treatment with Tau F1 decreasing in size and accelerating in proportion to changes in Na activation kinetics (Tau 5).

MB^+ appears to shift the gating currents in a parallel manner to the ionic currents suggesting a direct cause and effect relationship between the gating mechanism and ionic current generation. Supported in part by NIH Grant No. GM29263-01 and by Fellowship No. 1F32 ES05065-03.

*Rayner and Starkus "Kinetic analysis of I_{Na} and gating current in crayfish axons" Biophys. Abstr. 1982.

M-AM-Po94 SODIUM CURRENT FLUCTUATIONS IN AXON RESULTING FROM THERMAL AGITATION AND SHOT NOISE WITHIN THE CHANNEL. Franklin F. Offner, Technological Institute, Northwestern University, Evanston, Illinois 60201.

Fluctuations in current flowing thru the axonal membrane will result from the stochastic opening and closing of channel gates. Conti *et al (1)* have shown that if all the observed fluctuation noise results from this source, the Na^+ channel density can then be deduced from the zero frequency noise density of the noise power spectrum. There are two other obvious sources of channel noise: thermal agitation in the channel resistance (Johnson noise), and ion transit (shot) noise. These sources have previously been considered negligible, both because of their low amplitude and the short circuiting by the voltage clamp. If however one considers the m and h gates to be separate, noise is generated across their parallel resistance. Introducing this fluctuation into the Hodgkin-Huxley equation $I_{Na}=\bar{g}_{Na}h(V-V_{Na})$, the fluctuations are amplified by the steepness of dm^3/dV and dh/dV. This results in calculated noise equal within experimental error to that observed by Conti *et al (1)* and *(2)*, for low depolarizations. At higher depolarizations shot noise becomes significant and adds to the Johnson noise. With reasonable assumptions as to transit times, the sum accounts for all the observed noise over the full range of observations. It is concluded that Na^+ current fluctuations can give only a lower limit for Na^+ channel density.

(1) Conti,F., De Felice,L.J., and Wanke,E., *J. Physiol.* 248, 45, (1975).
(2) Conti,F., Hille,B., Neumcke,B., Nonner,W., and Stampfli,R., *J. Physiol.* 262, 699, (1976).

M-AM-Po95 EFFECTS OF OCTYLGUANIDINE ON NA CHANNEL GATING CURRENTS IN SQUID AXONS. G.E. Kirsch and J.Z. Yeh. Rutgers University, Piscatway, N.J., Northwestern University, Chicago, Il.

Octylguanidine (C8-G) is known from Na current (Ina) studies to block activated (open) channels and to simulate Na inactivation in pronase-treated axons. Using gating current (Ig) measurements in squid axons, we further characterized C8-G block and compared it to the h-gated inactivation. C8-G at 30 uM suppressed the peak of Ina to 57% of the control while having no effect on the ON Ig, as would be expected from a pure open channel blocker. In the presence of external 1 uM TTX, C8-G suppressed ON Ig to 66% of the control regardless whether permeant ions were present or not, suggesting that TTX stabilizes C8-G binding to its internal blocking site. Consistent with this view is that C8-G blockade of Na currents in pronase-treated axons was independent of external Na concentrations ranging from zero to 150 mM. The kinetics of the remaining ON Ig were accelerated and the voltage dependence of the total charge movement associated with it was shifted in the hyperpolarizing direction. Similar results on the ON Ig were observed in the pronase-treated axons, suggesting that the h gate is not required for C8-G action on Ig. The charge immobilization caused by C8-G was greater in the h gate-intact axon than in the pronase-treated axon. C8-G abolished the fast component of the OFF Ig; this component is resistant to the h-gated inactivation. This additional effect on the OFF Ig had a time course similar to C8-G blockade of Na currents. This indicates that the mechanism underlying these two phenomena may be closely linked. For example, both the effect on charge immobilization and C8-G induced blockade of Na currents reflect the blocking action of open channels by C8-G molecules. Our results support the notion that Na inactivation proceeds by occluding open channels by inactivating particles.

M-AM-Po96 ACTION POTENTIAL IN THE FERTILIZED EGG OF THE CTENOPHORE MNEMIOPSIS. M. E. Barish. Marine Biol. Lab., Woods Hole, MA, and Dept. of Physiology, Univ. of California, Los Angeles, CA.

Penetrations made with 30-50 MΩ electrodes in ASW with 30 mM Ca showed rest potentials (rp) between -70 and -90 mV. The slopes of the steady state I-V relations were linear over the range -120 to -50 mV, and gave input resistances of between 70 and 300 MΩ. The resting permeability was mainly to K ions, as shown by shifts in rp with changes in extracellular K concentration. The rp and I-V relation in the linear region were not affected by removal of extracellular Na (replaced by Tris) or Ca (replaced by Mg). The action potential (ap) shown below could be elicited by current injection. The duration of this example, about 6.5 min, was typical. The shape of the ap showed a number of characteristic features: (a) threshold at about -40 mV, (b) overshooting peak at about +20 to +40 mV, and (c) plateau at between +10 and +30 mV. The ap resulted mainly from an increase in permeability to Ca ions. Removal of external Na did not affect the amplitude of the peak or of the plateau. Reduction of external Ca reduced the amplitude of the peak, and both the peak and the plateau were abolished in Ca-free ASW. The ap was not affected by 2 mM Cd in the presence of Ca. In Ca- and Na-free ASW, the steady state I-V relation showed outward rectification at voltages above -20 mV. The initial rising phase of the ap appears to be driven by an inward current carried by Ca and possibly by Na as well. The later portion appears to depend solely on the inward movement of Ca ions. I believe this is the first report of excitability in an egg of the phylum Ctenophora. (Supported by the Grass Foundation, and USPHS NS07101, NS09012 and GM08676).

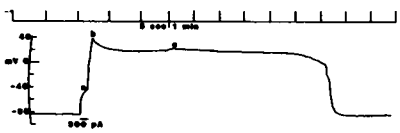

M-AM-Po97 ON EXPLORING THE BASIS FOR SLOW AND FAST OSCILLATIONS IN EXCITABLE MEMBRANES. Teresa Ree Chay, Dept. of Biological Sciences, University of Pittsburgh, Pittsburgh, PA 15260

By using a modified Eyring's multi-barrier kinetic model, we show quantitatively how the excitable membrane systems that contain immobilized enzymes (such as acetylcholinesterase) give rise to oscillations. These enzymes have the properties that they are inhibited by a substrate, that they have a pH activity profile of bell-shaped form, and that they produce an acid as one of the products. In consistency with the experimental observations in cellular excitations, these systems generate fast oscillations that are superimposed on a slow cycle, at certain external conditions.

This work was supported by NSF Grant 79 22483.

M-AM-Po98 MEASUREMENT AND INTERPRETATION OF MAGNETIC FIELDS FROM ACTION CURRENTS IN A SINGLE NERVE AXON. J.P. Wikswo, Jr., J.O. Palmer, J.P. Barach, and J.A. Freeman, (Intr. by E. Siegel) Dept. of Physics and Astronomy, and Dept. of Anatomy, Vanderbilt University, Nashville, TN 37235

We have used both superconducting and room-temperature current-to-voltage converters with low impedance room-temperature pick-up coils to measure the magnetic field associated with the action currents propagating along a single, isolated nerve axon. The nerve cord was dissected from 2 kg lobsters, and the miniature (1 mm I.D., 3 mm O.D. and 1 mm thick) toroidal pick-coil was placed around the cord. All nerve fibers except the medial axon were removed from the cord in the vicinity of the pick-up coil. Glass microelectrodes and miniature silver-silver chloride electrodes were used to record transmembrane and extracellular action potentials, respectively, at the pick-up coil. Upon stimulation of the nerve by a suction electrode, the magnetic field could be observed with a 15 to 1 signal to noise ratio. With signal averaging, the magnetic data are of sufficient quality to allow quantitative comparison with the magnetic field predicted from electric data using numerical solutions to Laplace's equation. These calculations demonstrate that the extracellular magnetic field is determined primarily by the axial, intracellular current. Examination of the core-conductor model demonstrates that extracellular magnetic measurements can be used to obtain the transmembrane action potential and the time-dependence of membrane conductivity without the use of microelectrodes. Magnetic recordings accompanied by either electric or magnetic subthreshold stimulation can be used to determine the length and time constants of an axon immersed in saline, also without microelectrodes.

Supported by ONR Contract N00014-80-C-0883 and an Alfred P. Sloan Research Fellowship.

M-AM-Po99 THE EFFECTS OF INTERNAL Na^+ AND H^+, EXTERNAL Ca^{++} AND OF MEMBRANE POTENTIAL ON Ca ENTRY IN SQUID AXONS, G. Vassort, T. Tiffert*, J. Whittembury** and L. J. Mullins*, Laboratorie de Physiologie Cellulaire Cardiaque, INSERM U-241 and CNRS LA89-03; Universite Paris Sud, F-91405, ORSAY, France, *Department of Biophysics, University of Maryland School of Medicine, Baltimore, **Laboratorio de Biofisica, Universidad Peruana Cayetano Heredia, Lima, Peru.

A comparison has been made of Ca entry during long depolarizing test pulses brought about by elevated K in seawater and measured either by arsenazo III or by aequorin. In the case of aequorin, light emission rose to high levels and then declined to a plateau; arsenazo III measurements showed, by contrast, that absorbance rose to a fixed level and remained there as long as depolarization persisted. This result suggests that there is an artifact to the described aequorin response. Measurements of the Ca entry with depolarization suggest that with saturating $[Na]_i$ as measured by Na-sensitive electrodes, Ca entry is half maximal if $[Ca]_o$ is 0.6 mM and that this value increases as $[Na]_i$ declines. Other experiments show that if $[Na]_i$ is kept at its normal value, Ca entry with depolarization is very small even if E_m approaches a value of zero. On the other hand, if $[Na]_i$ is elevated by stimulating the fiber in Na seawater, Ca entry begins at values of membrane potential of the order of -30 and increases greatly at values around zero. Ca entry with depolarization is negligible if $[Na]_i$ is made 10-15 mM; it is vastly enhanced when $[Na]_i$ is allowed to rise to 25-30 mM. Ca entry is half maximal when $[Na]_i$ is 25 mM. The application of 1-10 mM NH_4^+ in seawater to squid axons leads to an alkalinization of the axoplasm measured with pH-sensitive glass electrodes and to a Ca entry that is many-fold that of control fibers. The assumption is made that Ca entry is inhibited by acidification of axoplasm generated by Ca entry. Direct measurement of pH_i using phenol red confirms that Ca entry following depolarization leads to an acidification of axoplasm. Aided by Grants NIH 1 R01 NS17718-01; 5 P01 NS 14800-03 and NSF BNS-8006271.

M-AM-Po100 CHARACTERIZATION OF ACETYLCHOLINESTERASE (AChE) IN LOBSTER AXON PLASMA MEMBRANES. INHIBITION BY LOCAL ANESTHETICS. Judith K. Marquis and Erin E. Sahr, Dept. of Pharmacology and Experimental Therapeutics, Boston Univ. School of Medicine, Boston, MA 02118 (Sponsor: Norman I. Krinsky).

Axonal membrane vesicles were prepared from lobster (Homarus americanus) walking leg nerves. AChE activity of the vesicles is about 200 μmols ACh/hour/mg protein. The enzyme is a membrane protein that can be solubilized by lysolecithin but is inactivated by Triton X-100 and has previously been shown to be a glycoprotein by affinity chromatography on ConA-Sepharose 4B. The axonal enzyme contrasts most markedly with postsynaptic AChE in its poor inhibition by excess substrate. Axonal AChE was competitively blocked by eserine sulfate, activated by low Ca^{2+} concentrations (0.1 - 0.5 mM), inhibited by high Ca^{2+} (10 - 50 mM) and by local anesthetics. Terbium, a fluorescence probe of Ca^{2+}-binding sites, inhibited axonal AChE with an apparent K_i of approximately 0.5 mM. Propidium (1 μM) and decamethonium (1 μM), peripheral anionic site ligands in the synaptic enzyme, did not protect the axonal enzyme against inhibition by local anesthetics or against activation/inhibition by local anesthetics. Lidocaine, a tertiary amine, and its quaternary ammonium derivative QX-314 were equipotent enzyme inhibitors ($K_{i_{app}} \simeq 2$ - 3 mM) while the primary amine compound GX-HCl was totally inactive. (Supported in part by NIMH #35155).

M-AM-Po101 SMALL SIGNAL AND NOISE ANALYSIS OF K^+ CONDUCTANCE IN SINGLE MYELINATED NERVE FIBERS. T.D. Tsai and L.E. Moore, Department of Physiology, University of Texas Medical Branch, Galveston, Texas 77550.

The potassium conductance was activated by a conventional voltage clamp depolarization on which was superimposed either a second 5 mV step depolarization or a deterministic white noise command where the peak to peak magnitude was less than 5 mV. The step clamp data were fit by a sum of exponential functions. Comparison of relaxations in TTX Ringer's solution and high external potassium Ringer's showed a lengthening of the time constants in high K. In the high potassium the membrane shows a steady state negative K conductance which has admittance properties similar to those previously observed for a steady state negative sodium conductance. These data thus require a series RC branch rather than a RL branch to correctly model the linear relaxation data. The relaxation times determined from admittance spectra in high K were comparable to those determined in TTX Ringer. Spontaneous noise analysis under the same conditions as above showed an increased magnitude of the power spectra in high K as compared to TTX Ringer. The high K noise spectra were fit to a sum of two Lorentzians, one of which was comparable to the relaxation data.

This work was supported in part by NS 13520 and NS 13778.

M-AM-Po102 A VERSATILE PROGRAM FOR MODELING AXON KINETICS GENERATED BY COMPLEX MULTIPLE STATE REACTION SCHEMES. Heggeness, S.T. (Intr. by Guillory, R.) Dept. of Physiology, Univ. of Hawaii, Honolulu, HI 96822.

Multi-State kinetic analysis of ionic current and gating current records yields complex descriptive equations of the generalized form:

$$I_{(t)} = A_o + A_1 e^{-t/\lambda_1} + A_2 e^{-t/\lambda_2} \ldots + A_{N-1} e^{-t/\lambda_{N-1}}$$

for models containing N states, where A_x represents the weighting factor for each kinetic component, and λ represents the "system" time constant for each component. Each "system" time constant is a complex function of all the reaction rate constants of the entire reaction scheme. The testing of possible reaction schemes in order to evaluate their fit with experimental data is a difficult and time-consuming process. The development of analysis software is complicated in that it must be versatile enough to accommodate modifications in the kinetic scheme. This new program allows complete user control over the number of interactive states and the relationship between them, differences in reaction rate constants as a function of voltage, and the total number of states in the reaction matrix. Following the generation of data from hypothesized reaction matrices, this synthetic data can be subjected to kinetic analysis in a manner similar to experimental data. In this way, insights may be gained into the reaction scheme that underlies the time dependent membrane currents, and the feasibility of various model types can be analyzed and evaluated. Supported in part by NIH Grant No. GM29263-01 and by a grant from The South Pacific Commission.

M-AM-Po103 SODIUM GATING CURRENT AND SODIUM CURRENT IN FROG TWITCH MUSCLE FIBERS. N. L. Sizto, Dept. of Physiology, Univ. of Rochester, School of Medicine and Dentistry, Rochester, NY 14642.

A double vaseline gap voltage clamp was used to monitor the sodium current I_{Na} (no TTX) and gating current I_g (200 nM TTX) in the same cut bullfrog twitch muscle fibers detubulated by hypertonic glycerol treatment and held at -130 to-150 mV. External solution: Na Glutamate 10 mM, TMA Glutamate 110 mM, $CaCl_2$ 2 mM, Tris Maleate buffer 1 mM, 4-aminopyridine 2 mM. Internal solution: CsF 120 mM, Tris Maleate buffer 5 mM (5-10 C). The P/4 method was used for linear capacitative and leak correction. The sigmoidal Q vs. V curve for I_g was well described by the Boltzmann two-state model. No non-linear charge was observed for voltages more negative than -120 mV. Q_{ON} and Q_{OFF} were roughly equal for different test pulse amplitudes and durations for OFF voltages more negative than -130 mV, indicating relatively rapid return of all ON charge movement at these OFF voltages, After 60 µs ON I_g followed a single exponential time course (Rojas & Suarez-Isla, J. Physiol, 301, 46P, 1980) with time constant τ_{ON}. τ_m for I_{Na} was determined by fitting the current corrected for I_g with m^3h kinetics with a variable time delay and m^ah kinetics without a delay but with variable a. Both kinetics schemes gave good fits. τ_{ON} and τ_m (from m^3h with delay of about 90 µs) were identical (mean SEM $\tau_{ON}/\tau_m = 1.029 \pm 0.023$, N=22; monitored at many voltages from -40 to +30 mV in 2 fibers and at 0 or +20 mV in 3 other fibers). The simple kinetics for ON I_g and close similarity of τ_{ON} and τ_m suggests that the opening of Na channels in frog muscle surface membrane, unlike frog node of Ranvier (Neumcke et al, Pflugers Arch, 363, 193, 1976), may be determined by the movement of three identical and independent charged gating particles.

M-AM-Po103a ANOMALOUS EMISSION RESPONSES FROM SEVERAL RELATED CHARGE SHIFT PROBES OF MEMBRANE POTENTIAL. Logan L. Simpson and Leslie M. Loew, State University of New York at Binghamton, Binghamton, New York 13901

We have determined the potential dependent responses of the absorption and emission spectra for several dienyl analogs of the p-aminostyryl pyridinium chromophore. These response spectra are obtained from probe molecules bound to a hemispherical bilayer lipid membrane. The transmittance and absorption responses of these probes can generally be interpreted in terms of an electrochromic mechanism. The determination of the potential dependence of the emission spectrum involves fixing the excitation wavelength at a point where the transmittance response is zero, thus avoiding possible artifactual contributions from the potential dependence of the excitation spectrum. Nevertheless, there exists an asymmetry in the emission response which cannot be rationalized on the basis of electrochromism alone. These distortions from ideality probably are due to orientational relaxations of the membrane bound excited state during its lifetime.

(Supported by USPHS Grant GM25190 and a Research Career Development Award, CA00677, to LML.)

M-AM-Po104 ON MAGNETIC INDUCTION AT RESONANCE IN THE VISIBLE SPECTRUM OF TRANSITION METAL COMPOUNDS.
T. W. Barrett and F. L. Carter, Theoretical Chemistry Section, Code 6171, Surface Chemistry Branch, Chemistry Division, Naval Research Laboratory, Washington, DC 20375

We present experimental evidence from resonance Raman spectroscopy, normal Faraday effect and magnetic circular dichroism that a magnetic resonance (inverse Faraday effect) is elicited in transition metal compounds by circularly polarized visible light.[1] The incident circularly polarized light acts as an effective magnetic field and populates magnetic substates split in zero-field by crystal field energies. The result is a diamagnetic-paramagnetic switch, the explanation of which provides insight into the molecular dynamics of porphyrins and other transition metal compounds.

[1]Barrett, T. W., Proc. Molecular Electronic Devices Workshop, Editor: F. L. Carter, NRL Memorandum Report 4662 (1981) page 274.

M-AM-Po105 THE ERYTHROCYTE SEDIMENTATION RATE: THE EFFECT OF PARTICLE SHAPE.
L.C. Cerny, D.M. Stasiw and E.L. Cerny. Utica College of Syracuse University and the Masonic Medical Research Laboratory, Utica, NY.

The automatic sedimentimeter is designed to follow the entire settling process for a column of blood and also electronically generate the first derivative (Biorheology 14:145-9, 1977). In the present study, the erythrocyte sedimentation rate was examined using suspensions of spheres, discs and spindles. The results are interpreted in terms of concentration, cell volume and packing efficiency. A modified Stokes law is used to compare the theoretical calculations and experimental data (Biorheology 14:43-9, 1977). The reduced variables of distance and time were used to superimpose all the data on a single curve.

M-AM-Po106 INTERACTION OF FLUORESCENT SUGARS WITH AN UNIDENTIFIED SERUM MACROMOLECULE.
M.Derechin and D.A.Pragay,Departments of Biochemistry and Pathology,SUNY at Buffalo,3435 Main St., N.Y., 14214 and Erie County Medical Center,462 Grider St., Buffalo, N.Y. 14215.

After Lartey and Derechin (Anal.Biochem.1979,9,85) prepared the fluorescent sugar analog (FSA) DNS-glucosamine and showed differences in fluorescence after its interaction with,respectively,hexokinase and albumin, Derechin suggested (11th NERM,ACS,1981) the possible use of FSA's to establish the presence of molecules with sugar affinity for diagnostic purposes in cases in which such molecules are known to occur.With this in mind Derechin studied FSA interactions with sera from cancer and noncancer patients and normal volunteers (NERM,1981) and showed that cancer sera induced a lower fluorescence increase after mixing.We have now established that (i) sera from patients undergoing nonmalignant destructive processes (e.g. bone fractures,decubitus ulcers) behave as cancer sera in fluorescence intensity studies, (ii) the fluorescence changes after mixing FSA with serum arises from the FSA interaction with a hitherto unidentified serum macromolecule of relatively high molecular weight, and (iii) after electrophoresis at pH 8.6, this *serum interacting component (SIC)*, is located in a single band well behind the β-globulins and ahead of the γ-globulins,in an area unstained for protein.Using the fluorescence changes that occur uppon FSA-SIC interaction we have set up a continuous-automatic system to evaluate its possible use for cancer detection.Also,Derechin and Mattheis (to be published) using phase and modulation lifetime studies for heterogeneous systems (G.Weber,J.Phys.Chem.1981,85,949)identified distinctive FSA-SIC complexation patterns for malignant and nonmalignant destructive processes that may help in their differential diagnosis by laboratory means and are suitable for automation.These findings offer promising tools for cancer detection studies,particularly,for detecting the "cancer state" irrespective of cancer type or location

M-AM-Po107 EFFECT OF LIMITED ROTATIONAL MOTION ON SIMULATED CONVENTIONAL AND SATURATION TRANSFER EPR SPECTRA OF NITROXIDE SPIN LABELS. Kerry Lindahl and David D. Thomas, Dept. of Biochemistry, University of Minnesota Medical School, Minneapolis, MN 55455.

EPR theory for nitroxide spin labels is well understood for isotropic Brownian rotational diffusion, but only recently have there been theoretical investigations into the equally realistic case of limited rotational motion. Restricted motion has been postulated for the dynamics of muscle proteins and some proteins in membranes. The type of motion studied was the wobbling, of nitroxide spin labels, within a cone of angular width $\Delta\theta$ (for isotropic motion, $\Delta\theta$ is greater than or equal to 90°).

Computer simulations involved solving the Bloch equations, with a diffusion term and appropriate boundary conditions, for different magnetization components, harmonics, and phases. When $\Delta\theta \gtrsim 90°$, the spectrum corresponds to isotropic rotational motion, where $D=1/(6\tau_c)$. D is the rotational diffusion coefficient, and τ_c is the rotational correlation time. Decreasing $\Delta\theta$ produces a spectrum appearing like that for isotropic motion, but with a decreased apparent diffusion coefficient, D_{app}. This effect is large for conventional EPR spectra, i.e., these spectra are insensitive to small angle rotational motion. For example, for $\Delta\theta=15°$ and $D=10^9$ sec., $D_{app} \lesssim 10^7$ sec. This effect is smaller for STEPR, i.e., STEPR spectra are more sensitive to small angle rotational motion.

M-AM-Po108 ANALYSIS OF WAVEFORMS OF BIOLOGIC TIME SERIES, C. M. Winget*, N. W. Hetherington**, and L. S. Rosenblatt**, *NASA-Ames Research Center, Moffett Field, CA 94305, **Geneticon, 748 Minert Rd., Walnut Creek, CA 94598.

A model for analyzing asymmetric biologic rhythm data, non-stationary in time, with a changing period for successive cycles of the time series is presented. Using methods from the finite calculus we estimate secants from 5 successive data (Y) and obtain the derivatives (ΔY). Y plotted against ΔY will produce a closed configuration in the phase plane if the time series is rhythmic. The number of (equispaced) data to close the loop is an estimate of the period. We may also determine a series of physiologic states from this configuration which are divorced from sidereal time and are measures internal time (e.g. circadian). For asymetric waveforms angular velocity is not constant and changes in the waveform can be related to changes in angular velocity. The method also allows the detection of short periodicities in the data. It is also possible to gain insight into the control system governing the rhythm. We complete the second derivative (Δ^2Y), the acceleration, which when plotted against ΔY provides us with the trajectory of the acceleration and with landmarks which can be related to physiologic function. Analyses of human data (n=28; [illegible]) have provided evidence for a loose and tight control systems in thermoregulation.

M-AM-Po109 USE OF A SEMI-PERMEABLE MEMBRANE POUCH FOR DIALYSIS PROCESSING OF CRYOPRESERVED RED BLOOD CELLS. A. Zelman and D. Gisser, Rensselaer Polytechnic Institute, Troy, N.Y.

The cryopreservation of red blood cells requires a 3-4 M concentration of glycerol to prevent freezing injury. Living cells may be frozen for several years, thawed, and with glycerol removed, administered in place of fresh red blood cells. Present techniques for removal of glycerol are labor intensive, osmotically harsh to the fragile RBC, costly and do not insure sterility of the blood.

Our approach places the blood in a pouch composed of heat-sealed, polycarbonate, semi-permeable membrane material. Glycerol can be added or removed from the blood by dialysis through the pouch itself which is an absolute barrier to pyrogens, viruses, and bacteria. Glycerol is added to the blood pouch by increasing exponentially the concentration of glycerol in the dialysate up to 3.5 M. The blood pouch may be stored at -80°C indefinitely. The cells may be thawed and glycerol removed while the RBC's remain sterile in the pouch. The rate at which glycerol is removed from the RBC is controlled by adjusting the flow rate and electrolyte concentration of the dialysate flushing the bag. As glycerol is removed, NaCl is added to protect the cells from osmotic damage. Subsequently the NaCl is removed by further dialysis. Residual glycerol can be lowered to levels suitable for reinfusion (<200 mosm) in 20 min and reduced to negligible levels in 30 min.

These methods offer simplicity, potential for processing multiple units without the possibility of cross contamination, a completely sterile procedure, negligible cell loss and/or damage due to osmotic shock and oxygenate the RBC to greater than 90% saturation. These procedures can easily be automated, greatly reducing technician time required for deglycerolization.

Supported by PHS grant NIH-HL-24466.

M-AM-Po110 THE USE OF QUASI-ELASTIC LIGHT SCATTERING TO PROBE THE CELLULAR MOTION OF CHLAMYDOMONAS REINHARDTII. T.J.Racey* and F.R.Hallett, Biophysics Interdepartmental Group, Department of Physics, University of Guelph, Guelph, Ontario, Canada N1G 2W1

Quasi-elastic light scattering (QELS) has proven in the past to be a useful and interesting tool for examining parameters of motion for various microbiological objects such as: human spermatozoa[1], bull spermatozoa[2], E. coli[3] and Euglena gracilis[4]. In this work we have investigated a common algae, Chlamydomonas reinhardtii, to compare the relative average swimming speeds of the wild type cells (ATCC #18798) with a colchicine resistant (colch^r-1) mutant (ATCC #30552), and a backwards swimming (RL-10) mutant (obtained from S.Nakamura[5]) using QELS. We have also been successful in using this technique to examine the variations in the average swimming speeds of the wild type cells as a function of their temperature, and have been able to illustrate the variations in the average swimming speed as a function of the external concentration of Mg^{++}, Ca^{++} and Ni^{++} in their environment. The speed of the QELS technique allowed us to follow fairly rapid changes in motility which arose after a chemical or physical perturbation. A mathematical model of the swimming cell based upon cinematographically observed oscillating-translational motion of C. reinhardtii has been used to analyse the QELS data quantitatively. (1) Jouannet et al. 1977, Andrologica 9:36;(2) Craig et al. 1979, Biophys. J. 28:457;(3) Holz and Chen, 1978, Applied Optics 17:3197;(4) Ascoli et al. 1978, Biophys. J. 24:585;(5) Nakamura, 1979, Exp. Cell Res. 123:441.

M-AM-Po111 DEVELOPMENT OF LONG OPTICAL PATH LENGTH THIN LAYER SPECTROELECTROCHEMICAL CELLS. Michael J. Simone, Ralph A. Magnotti, William R. Heineman and George P. Kreishman. Department of Chemistry, University of Cincinnati, Cincinnati, Ohio 45221.

The utility of optically transparent thin layer electrodes has been demonstrated for the study of both small electroactive molecules as well as electroactive proteins. The main draw-back of many of these techniques has been the extremely short optical path length which requires relatively high concentrations of the analyte. Under conditions where only small amounts of sample are available or where low concentrations are necessary for analysis, the practical use of these techniques is limited. The development of novel designs which have relatively long optical path lengths and are suitable for use with absorbance and fluorescence spectrophotometers have made low concentration spectroelectrochemical experiments possible. Experiments utilizing the cells with o-tolidine and horse heart cytochrome c at μM concentrations will be discussed.

M-AM-Po112 THE APPLICATION OF A NOVEL DIALYSIS FERMENTOR DESIGN TO THE PROBLEM OF METABOLITE INHIBITION RELIEF IN YEAST. M.E. Himmel and J.H. Janssens, Biotechnology Branch, Solar Energy Research Institute, Golden, CO 80401.

Conventional ethanol fermentation is limited by the inhibitory effect of the product which decreases the rate of ethanol production and cell biomass concentration. In large scale alcoholic fermentations the vacuum fermentation process is a possible solution, however the energy cost is a major disadvantage. In order to remove the ethanol during cultivation the method to be employed would necessarily be selective for ethanol and capable of being operated aseptically.

The method of dialysis fermentation offers a suitable solution to these problems in theory; however, there are currently no analytical dialysis fermentors available commercially. We have designed and constructed a dialysis fermentor consisting of concentric tubular dialysis membranes. This system is capable of independent control of component operations, repeated autoclaving and continuous operation. In this paper we present the design and apparatus with the method of operation and some basic considerations of continuous ethanol production. Experimental results from actual yeast fermentation are discussed.

This technology is ultimately suitable to any fermentation problem where the terminal product is inhibitory.

M-AM-Po113 COMPARATIVE ANALYSIS OF SEVERAL DOUBLE- AND TRIPLE-GAP VOLTAGE CLAMP CIRCUITS. Gunter N. Franz and David G. Frazer. Dept. of Phvsiology, West Virginia University Medical Center and Lab. Investig. Branch, Div. of Respir. Dis. Studies, NIOSH/CDC/PHS Dept. of Human Health Service, Morgantown, WV 26506

Topological analysis reveals that several well-known voltage clamps (VC) using double sucrose gaps or triple vaseline seals and a single primary feedback loop can be reduced to the complementary configurations of the inverting (I) and noniverting (N) operational amplifier. One configuration can be switched to the other by exchanging the connections to ground and VC command source for the appropriate pools. In both cases the internal fiber resistance is in the feedback loop. Examples of the "I" configuration are the circuits by Bergman and Stämpfli (1966), Rougier et al. (1968), and Nonner (1969). Typical "N" configurations are those of Poindessault et al. (1976) and, with appropriate modification, of Julian et al. (1962). These two classes of VC circuits are converted into current clamps (CC) by interchanging pool connections so that the membrane impedance is in the feedback loop. The "I" version is then the CC of Dodge and Frankenhaeuser (1958). The "N" version is probably new. These CC circuits can be expanded into VC circuits by replacing the CC command sources with amplifiers forming a second feedback loop. The "I" version of this dual loop VC is the classical circuit of Dodge and Frankenhaeuser (1958). The "N" version is a new circuit. We also developed a VC circuit of quite different topology based on the boot strap principle. Our analysis of the circuits included DC behaviour, open-loop gain, influence of amplifier characteristics, and series resistance compensation.

M-AM-Po114 NANOSECOND EXPOSURE X-RAY DIFFRACTION PATTERNS FROM BIOLOGICAL SPECIMENS USING A LASER PLASMA SOURCE* J. M. Forsyth and R. D. Frankel, Intr. by William A. Bernhard, Laboratory for Laser Energetics, University of Rochester, Rochester, NY 14623

We describe a facility for time-resolved x-ray diffraction studies of biological systems which has been constructed based on the use of focussed high peak power, frequency converted nd+3:glass laser pulses to produce a high energy density plasma x-ray source. Using image intensifier aided detection with a toroidal focussing x-ray diffraction camera, complete fiber or powder diffraction patterns may be recorded from a single laser pulse. A digital vidicon detection system has been assembled from commercial components which can acquire, process and Fourier transform the diffraction patterns during the 30 minute laser shot cycle. The pulsed x-ray source has been synchronized to a laser photostimulus system enabling us to perform structural kinetic studies of a wide variety of photoactive systems.

*Work supported, in part, by the National Institute of Health, the National Science Foundation and the Laboratory for Laser Energetics.

M-AM-Po115 TIME RESOLVED LASER MICROSPECTROFLUORIMETER. Salvador M. Fernandez. (Intr. by R.I. Sha'afi. University of Connecticut Health Center, Farmington, CT 06032.

An instrument has been developed to perform time-resolved fluorescence relaxation measurements on single cells through a fluorescence microscope. The instrument is equipped with a picosecond pulsed laser source, image intensification, digital image processing, and time-correlated single photon counting capabilities. At the heart of the apparatus is a Zeiss fluorescence microscope equipped with a vertical illuminator. The laser system is a synchronously pumped mode-locked cavity-dumped tunable dye laser system which employs an 18 watt krypton laser as the pump source (Spectra Physics). The laser can be operated either in CW mode for steady state applications (imaging) or in pulsed mode for time-resolved studies. Corresponding to these two modes of excitation, the microscope is equipped with two different detection systems: a SIT camera interfaced to a Quantex digital image processor or a monochromator coupled to a refrigerated photomultiplier tube connected to timing electronics. Selection of the appropriate detection system is accomplished by means of a beam splitter. Data generated by either mode of operation can be transferred to a computer for processing and analysis.

Time-resolved spectra, fluorescence lifetimes and decays of emission anisotropy can be obtained from single cells or small regions of single cells in very short times, making possible the study of a variety of dymamic cellular processes in live cells in real time. In addition, a beam steering device can be used to direct the laser beam onto a macroscopic sample compartment(SLM Instruments) where similar measurements can be made from samples contained in cuvettes.

This research was supported by grant GM27524 from the N.I.H.

M-AM-Po116 SIMULATION OF INTERNAL DIALYSIS OF GIANT AXONS. Lyle W. Horn. Temple Univ. Phila. 19140

A numerical analysis of solute distribution in internally dialyzed axons was done taking account of the complete geometry, end effects, finite dialysis solution flow, and physical properties of axoplasm and dialysis tubing. Evaluation of the method focused on events occurring within a typical experimental time period. Control of nonmetabolized solute concentration at the cell membrane over at least 92% of the dialyzed zone is greater than 99% ideal for membrane permeabilities less than 10^{-6} cm/sec. Undialyzed ends do not affect control or equilibration time provided the ratio of the dialyzed length to axoplasm thickness exceeds 20. Most solutes in a mixture will equilibrate at about the same time, but strongly bound solutes are much slower. A 1000 fold reduction of solute concentration over 90% of the dialysis zone is feasible. Solute control is effective even at low dialysis solution flow. The dialysis tubing wall is an equilibration rate limiting step when the diffusion time scale ratio (wall/axoplasm) exceeds 0.08. Equilibration time is linearly (approximately) related to the mean transit time of dialysis fluid through the dialysis zone, but the flow sensitivity (slope) varies with the wall/axoplasm diffusion time scale ratio. Maximum flow sensitivity occurs at an intermediate ratio. Development of end effects in efflux experiments is very slow. For most solutes end effects are small for the first 30 min of an influx, but rise rapidly thereafter. Influx end effects remain small for strongly bound solutes. Results confirm the general assessments of the method based on years of application. (Supported by NIH Grant NS 14569 and funds from the Univ. Maryland Computer Science Center).

M-AM-Po117 ENZYMIC HYDROLYSIS OF INTRAMOLECULARLY QUENCHED FLUOROGENIC SUBSTRATES FOR MONITORING HOMOGENEOUS COMPETITIVE PROTEIN BINDING REACTIONS. Thomas M. Li and John F. Burd*, Ames Division, Miles Laboratories, Inc., Elkhart, IN 46515.

We describe a new method for measuring analytes in competitive binding reactions. This method uses an enzyme substrate molecule that contains a fluorophore component, a quencher component, and the analyte. The fluorophore and quencher are covalently connected with a chain that contains a bond that is susceptible to enzymatic hydrolysis. The method was tested using flavin-N^6-(6-Aminohexyl-theophylline) adenine dinucleotide (FAD-Theophylline) as the intramolecularly quenched fluorogenic substrate. The fluorescence of the flavin mononucleotide (FMN) is quenched by the adenosine monophosphate (AMP) portion of this molecule. Hydrolysis of FAD-Theophylline by nucleotide pyrophosphatase produces FMN and AMP-Theophylline yielding the expected fluorescence due to the FMN. Antibody to theophylline binds to FAD-Theophylline and inhibits the enzymatic hydrolysis. Competitive binding reactions can therefore be established using a constant level of FAD-Theophylline and a limiting amount of antibody to measure theophylline levels in unknown samples. The theophylline in the unknown sample competes with the FAD-Theophylline for the antibody binding sites. Only the FAD-Theophylline not bound to antibody is available for enzymatic hydrolysis. Therefore, the fluorescence produced is proportional to the level of theophylline in the unknown sample. The assay is quick and convenient to perform and does not require separation procedures.

M-AM-Po118 ONE STEP DETERMINATION OF HYDROGEN TRANSFER STEREOSPECIFICITY OF NICOTINAMIDE NUCLEOTIDE LINKED OXIDOREDUCTASES. Shan S. Wong, Department of Chemistry, University of Lowell, Lowell, Mass 01854

A simple one-step method has been development for the determination of hydrogen transfer stereospecificity of nicotinamide nucleotide-linked oxidoreductases by using NMR technique. For NAD^+-linked oxidoreductases, alcohol [EC 1.1.1.1] and lipoamide [EC 1.6.4.3] dehydrogenases whose stereospecificities are known are employed to prepare stereospecifically deuterated reduced nicotinamide adenine dinucleotide which is immediately reoxidized in situ in a NMR tube by the enzyme under investigation. For $NADP^+$ stereospecificity determinations, alcohol dehydrogenase [EC 1.1.1.2] and glutathione reductase [EC 1.6.4.2] are used. The reoxidized coenzyme of the coupled reactions is analyzed for its deuterium content by NMR. The presence and absence of the absorption band due to the hydrogen or deuterium, respectively, at the 4-position of the nicotinamide ring is used to diagnose the stereospecificity of the test enzyme. Alternatively, the reduced coenzyme formed by the test enzyme may be analyzed by two enzymes of different stereospecificities. Application of this direct coupling method to α-keto acid dehydrogenase complexes revealed that both pyruvate and α-ketoglutarate dehydrogenase complexes were B-side stereospecific for NAD^+. With $NADP^+$, L-lactate, malic and glycerate dehydrogenases showed A-side stereospecificity, whereas α-glycerophosphate and glutamate dehydrogenases were B-side stereospecific.

M-AM-Po119 OPTIMIZATION AND COMPARISON OF SEPARATION PROCESSES. W.D. Corry*, G.V.F. Seaman and Duane A. Szafron*, Department of Neurology, Oregon Health Sciences University, and Department of Mathematics, Portland State University, Portland, Oregon 97201

A method for quantitatively evaluating the success of separation processes is presented. These processes are regarded as methods by which objects are ordered with respect to some set of properties. When a separation process orders a collection of n different types of objects into n fractions, the distribution of the different types of objects throughout all of the fractions can be described by an n by n matrix, A. An ideal separation process is characterized by an identity matrix. The success of a separation process can be characterized by a quantity called its inefficiency, which is obtained by summing investigator assigned penalties for sorting errors. Calculation of this inefficiency requires a knowledge of the composition of the fractions created by the process. When this information is unknown it can be estimated by the following process. After the initial sorting process, the objects in each fraction are labelled to denote their membership in that fraction. They are then remixed, resorted by the same process as before and the distribution of labelled objects is determined. The distribution of labelled objects is then used to create a new matrix, B, which can be used to approximate the original matrix since B = Transpose(A) times A. This approximation and simulation studies of the probable distributions of A which could give rise to B are then used to estimate the true inefficiency of the separation process. (Supported by NIH Grants HL 18284 and HL 24374.)

M-AM-Po120 DETERMINATION OF CHARGE AND MOLECULAR WEIGHT OF POLYELECTROLYTES BY SEDIMENTATION. Emory H. Braswell. University of Connecticut, Storrs, Connecticut 06268

It is well known that even in the presence of salt the determination of the molecular weight (MW) of a polyelectrolyte yields results that are lower than the true MW. The amount of this error depends on the charge nature of the salt, the relative values of $\bar{v}$ for the salt and the polyelectrolyte, and the actual (as opposed to stoichometric) charge on the polyelectrolyte. Casassa and Eisenberg showed that during dialysis of a polyelectrolyte in a solvent containing a dialyzable salt against the same solvent, a quantity of the salt is "pumped" across the membrane from the polyelectrolyte solution to the salt solution. Since this increase in salt concentration is directly related to the actual charge on the polyelectrolyte, one can calculate the true MW from sedimentation data. This paper presents a method by which the dialysis equilibrium is performed in the ultracentrifuge cell by centrifuging at high speed so that a boundary is rapidly formed. As with the dialysis membrane salt will be "pumped" across the boundary into the supernatent region. The increase in salt concentration can be detected as a decrease in the refractive index difference between the solution and the solvent (measured before the experiment) and that across the boundary. This technique has a clear advantage over the conventional dialysis experiment. For a number of reasons dialysis equilibrium is established quite rapidly under these conditions resulting in measurements under an hour. The centrifuge can then be slowed and the experiment continued to equilibrium for the purpose of determining the MW. Data is presented from studies with dextran sulfate (MW≈200000) and heparin (MW≈20000), and corrections and precautions are discussed.

M-AM-Po121 PROGRAMS FOR DESK-TOP ANALOG AND DIGITAL COMPUTERS TO ANALYZE PERMEABILITY DATA. H.G. Hempling, Department of Physiology, Medical Univ. Of S.Carolina, Charleston, S.C.

In the course of kinetic analyses of the permeability of cell membranes to water, non-electrolytes, and electrolytes, we have prepared a number of programs to use with desk-top analog and digital computers. Details do not always appear in the literature because of limited space. Therefore we have prepared listings and patching diagrams for distribution. Included are:

1. Interfacing a particle size analyzer to analog and digital components to measure changes in cell volume with time.
2. Solution of equations of Kedem and Katchalsky to obtain the hydraulic coefficient, the reflection coefficient, and the solute permeability coefficient.
3. Calculating the hydraulic coefficient from the equation of Lucke, Hartline, and McCutcheon.
4. Optimizing routines to fit data to two compartment flux models in series and in parallel.

M-AM-Po122 ELECTROCHEMICAL METHODS FOR THE DETERMINATION OF PROTEIN CONCENTRATION. COLLAGEN AND ALBUMIN AT THE MICROGRAM LEVEL. Matthew J. Doyle, George W. Dombi, William R. Heineman and H. Brian Halsall, Department of Chemistry, University of Cincinnati, Cincinnati, Ohio 45221

Due predominantly to a lack of appropriate chromophores, collagen is a particularly difficult protein to quantitate at low concentrations. Collagen does chelate lead, and this may be detected by differential pulse polarography at a dropping mercury electrode. Chelation increases from pH 1 to pH 5.5, where the redox process has the lowest detection limit. Lead chelated to collagen reduces at -594 mV at pH 5.5, and at saturation the reduction peak is directly proportional to the collagen concentration, which can therefore be readily quantitated. Saturation is achieved by adding excess lead, which reduces at -422 mV and therefore doesn't interfere. Collagen is quantitatable to 6 μg/ml. An alternative approach used the adsorptive properties of proteins on mercury drops to impede access to the drop of the reducible species In^{3+}. Human serum albumin was used as a model for this concept. The cathodic reduction wave (-480 mV vs. Ag/AgCl) of 10^{-4} M In^{3+} in 0.1 M citrate undergoes a progressive decrease in peak current as the concentration of albumin present increases. Albumin concentrations as low as 20 μg/ml could be routinely quantitated by this method. The isoelectric point of the protein dictates the pH dependence of the assay and the degree of charge interaction occurring at the electrode interface.

Supported by NIH Grant AI 16753.

M-AM-Po123 DIRECT OBSERVATION OF RESOLVED RESONANCES FROM INTRA- AND EXTRACELLULAR SODIUM-23 IONS IN NMR STUDIES OF INTACT CELLS AND TISSUES USING DYSPROSIUM(III) TRIPOLYPHOSPHATE AS PARAMAGNETIC SHIFT REAGENT. Raj K. Gupta and Pratima Gupta*. Institute for Cancer Research, Phila., PA 19111.

Sodium ion fluxes in animal cells appear to play an important role in a variety of fundamental processes associated with cellular activity. It is of considerable physiological interest to study intra- and extracellular Na^+ ions and their fluxes across the plasma membrane in intact cells and tissues under various conditions by the noninvasive technique of NMR spectroscopy. Unfortunately, the sodium resonances of intra- and extracellular Na^+ ions in cell suspensions occur at the same frequency in the spectrum, and this lack of spectral resolution has so far limited the applicability of the NMR technique to the study of the state of intracellular Na^+ ion. Because of our continuing interest in developing applications of NMR for the study of the role of ions in various cellular phenomena, we have been exploring ways of resolving the resonances of intra- and extracellular Na^+ ions in the NMR spectrum. After numerous fruitless trials, we have discovered that the complex of dysprosium(III) with tripolyphosphate ($Dy(III)(PPP_i)_2$) is an efficient paramagnetic NMR shift reagent that allows direct observation of resolved resonances from intra- and extracellular Na^+ ions in physiological suspension of cells. We report the discovery of this reagent and examples of its use with the human red blood cells and frog skeletal muscle. Since this paramagnetic reagent provides effective resonance separation at relatively low concentrations ($\sim$ 2 ppm with 1 mM Dy(III) at physiological levels of extracellular Na^+ and pH), it should be widely useful in sodium-23 NMR studies of intact cells and tissues. (Supported by USPHS. NIH Grant AM-19454).

M-AM-Po124 MEASUREMENT OF NEMATODE MOTION PARAMETERS BY DYNAMIC LASER LIGHT SCATTERING. Victor K-H. Chen* and W.F. Hieb*. *Department of Biophysical Sciences and Division of Cell and Molecular Biology, State University of New York At Buffalo, Buffalo, New York 14214(Intr.by R.A.Spangler)

Behavioral and genetic analysis with Caenorhabditis elegans have resulted in a search for new methods for measuring the movement behavior of nematodes. We have found that nematode movement parameters can be measured by dynamic laser light scattering. This technique makes it possible to monitor complex movements in a relatively short period of time with great accuracy and sensitivity.

Intial experiments were carried out with Turbatrix aceti because of its rapid motion and its swimming ability in liquid medium. A relative high concentraction(10^4/cc.) of worms in liquid medium was illuminated with a 5mW. helium-neon laser beam. Scattered light was detected by a photomultipler in a photon counting arrangement. The resulting was fed into a digital"autocorrelator" which computes the autocorrelation function of the worms motion.

The autocorrelation function yields directly the major movement frequencies of the worms. Some of the frequencies may be the result of varying rates in the different parts of the organism. Alteration of behavioral conditions or changes inthe physiological state resulted in the appearence of distinct frequency patterns. Therefore this method makes possible the quantitative and qualita tive measurement of movement parameters in worm populations within a period of a few minutes. We have examined the effect of oxygen level, nematode size and age and several anthelmenthics on te response to dynamic laser light scattering, as well as that of different species- i.e.,C. briggsae P. silusiae.

M-AM-Po125 HIGH RESOLUTION ELEMENTAL IMAGING. H. Shuman, A.V. Somlyo and A.P. Somlyo. Pennsylvania Muscle Institute, University of Pennsylvania Medical School, B42 Anatomy-Chemistry Building, Philadelphia, Pennsylvania 19104.

Energy filtered electron microscopy and x-ray mapping are suitable for the visualization of the elemental composition of materials at electron microscopic resolution (1-3). We have developed a single sector magnetic spectrometer and used it to form filtered images of ferritin molecules using electrons scattered from the Fe-$M_{2,3}$ and C-K characteristic absorption edges. The 7.5nm iron core and 12nm protein shell are clearly distinguished. The minimum detectable mass is estimated from these images to be $.84 \times 10^{-20}$g. for Fe with an electron dose of 18 coul/cm^2. Filtered images using the Ca-$L_{2,3}$ edge scattered electrons shows calcium localized in the inner core and outer cortex of B. coagulans spore, also shown in X-ray maps in (4), and in the organelles of saponin-skinned, Ca-loaded vascular smooth muscle. Electron probe x-ray mapping of normal resting frog striated muscle shows Ca localized in the terminal cisternae. The best resolution obtained in x-rays maps of Mo-stained catalase crystals based on two dimensional Fourier transforms is approximately 6.7nm. The ultimate sensitivity and resolution obtainable with electron energy loss imaging can be better than with x-ray mapping. The use of this single sector spectrometer has the advantage that, unlike other imaging systems, it can be used without modification of the high vacuum column.

1. Isaacson, M. and D. Johnson. Ultramicroscopy 2: 33, 1979.
2. Ottensmeyer, F.P. and D.P.Bazett-Jones. Science 211: 169, 1981.
3. Somlyo, A.P., A.V. Somlyo, H. Shuman and M. Stewart. Scan. Elect. Micros., II Sem. 711, 1979.
4. Stewart, M., A.P. Somlyo, A.V. Somlyo, H. Shuman, J.A. Lindsay and W.G. Murrell. J. Bact. 147: 670, 1981.

This work was supported by HL-15835 to the Pennsylvania Muscle Institute.

M-AM-Po126 HIGH SENSITIVITY AND RESOLUTION APPROACH TO THE QUANTITATIVE DETERMINATION OF SIZE AND NUMBER OF PLATELET AGGREGATES COMBINING RESISTIVE PULSE SPECTROSCOPY AND GLUTARALDEHYDE FIXATION. E.N. Serrallach, S. Simmons, C.P. Emerson and C.R. Valeri. Naval Blood Research Laboratory, Boston University School of Medicine, Boston, MA, U.S.A.

Resistive Pulse Spectroscopy (RPS) is a recent technological development. The Coulter Channelyzer model H4 with logarithmic volume scale expansion provides accurate histograms (VDH) of the number versus volume of cells (including platelets), cell aggregates and cell fragments in blood. It collects in 1 minute information re 100,000 particles in an adjustable volume range including 4 logarithmic cycles - in our case, from about 0.5 to 5000 μm^3. Count and volume information is stored in 256 channels. 1% glutaraldehyde (GA), a widely used crosslinking reagent for fixing proteins, preserves the aggregation state. Combining RPS and employing GA fixation to terminate the aggregation reaction at selected times following the addition of ADP, we studied the changes in the VDH as a result of incubating platelet-rich plasma with 10^{-5} to 10^{-8} M ADP. The analysis of the VDH profiles included three volume windows. The first corresponded to platelet fragments up to 1 μm^3; the second represented the main platelet peak, characterized by normal distribution with volumes between 1 and 40 μm^3. The third, displaying a broad peak, contained microaggregates up to 5000 μm^3. At 10^{-7} M ADP, about 5% of the platelets aggregated; at 10^{-6} M ADP, up to 80%. The size of the microaggregates was ADP concentration dependent, exceeding 5000 μm^3 at 10^{-5} M ADP. This protocol provides a 16-fold improvement in platelet sizing and a 5-fold increase in sensitivity for detecting platelet activation. The same protocol is applicable to studies of platelet behavior during storage and on exposure to cryoprotectants and anticoagulants.

M-AM-Po127 INTERACTION OF A FLUORESCENT HEXOSE ANALOG WITH RAT ADIPOCYTES. M. DiPaola[*#], F. Maxfield[*], and R. Murphy[#], Department of Pharmacology(*) and Chemistry (#), New York University, New York, NY 10003

The fluorescent hexose analogue dansyl-glucosamine was prepared by reaction of dansyl chloride with glucosamine hydrochloride. When added to freshly isolated rat adipocytes (1-5 x 10^6 cells/mL) in the micromolar range (1-100 µM) dansyl-glucosamine showed a spectral broadening in its emission spectrum. Analysis of the emission band disclosed two components corresponding to 460 nm and 505 nm. The intensity of the 505 nm band increased linearly with increasing dansyl-glucosamine concentration, while the intensity of the 460 nm band saturated in the micromolar range (K_d=19µM). If the adipocytes were incubated in the presence of phloretin (0.10 mM) prior to the addition of dansyl-glucosamine (25 µM), the intensity of the 460 nm band was reduced by 4-5 fold compared to cells without phloretin, while if the cells were pretreated with insulin (100 nM) the intensity at 460 nm was increased by 1-5 fold. Fluorescence depolarization studies of dansyl-glucosamine in the presence of adipocytes revealed that the emission at 460 nm was polarized with P≅ 0.23. If the adipocytes were pretreated with insulin (100 nM) the polarization decreased to~0.06. Investigation of the kinetics of dansyl-glucosamine binding showed that the association rate constant (k_1) and the dissociation rate constant (k_{-1}) were 1.05 x 10^4 $M^{-1}sec^{-1}$ and 0.51 sec^{-1} , respectively; when cells were pretreated with insulin k_1 and k_{-1} were found to be 2.9 x 10^4 $M^{-1}sec^{-1}$ and 1.58 sec^{-1}, respectively . Dansyl glucosamine was found to competitively inhibit (K_i = 0.035 mM) the facilitated transport of [^{3}H]-3-O-methyl-D-Glucose in rat adipocytes. These data suggest that dansyl-glucosamine may interact with the adipocyte hexose transporter.

M-AM-Po128 POISSON-BOLTZMANN CELL MODEL THERMODYNAMICS OF DILUTE SOLUTIONS OF ROD-LIKE POLYIONS. Charles F. Anderson, Barbara K. Klein, and M. Thomas Record, Jr., Department of Chemistry, University of Wisconsin, Madison 53706

New closed form expressions for the thermodynamic coefficients describing nonideality in solutions containing rod-like polyions and arbitrary amounts of added salt have been derived from the Poisson-Boltzmann cell model, as formulated by Marcus [J. Chem. Phys. 23, 1057 (1955]. The expression for the Donnan coefficient, Γ, depends on α, the extent of counterion dissociation, on ξ, proportional to the mean structural charge density along the polyion axis, and on S_a, proportional to the sum of the local activities of the small ions at the polyion surface. Various other ways of defining the thermodynamic interaction between small ions and a rod-like polyion lead to PB cell model expressions identical to that derived for Γ. The polyion contributions to the osmotic coefficient of the solvent and the activity coefficient of the added salt are simple functions of α, ξ, S_a and X, the ratio of added salt to polyion monomer. At low salt concentrations each of the thermodynamic coefficients is governed by the limiting forms of S_a, which differ according to the magnitude of $\alpha\xi$ relative to unity. The resulting Poisson-Boltzmann "limiting law" expressions correspond closely to those obtained by Manning using the hypothesis of counterion condensation. Based on the PB expressions for the thermodynamic interaction of small ions with rod-like polyions, new equations describing the salt-dependence of the helix-coil transitions of nucleic acids are derived and applied to experimental data. (Work supported by NSF grants PCM 79-04607 and NIH grant GM-23467)

M-AM-Po129 DENSITY GRADIENT ELECTROPHORETIC SEPARATION OF LIVING MAMMALIAN CELLS: EFFECT OF POSITION IN THE CELL CYCLE. L. D. Plank, M. E. Kunze, C. Goolsby and P. Todd. The Pennsylvania State University, 403 Althouse Laboratory, University Park, PA 16802.

Reports on the change of mammalian cell electrophoretic mobility through the cell cycle contain various results, some indicating no changes and others indicating significant changes, usually in cells from cultures subjected to biochemical synchronizing procedures. Experiments were performed in which asynchronous cell populations were subjected to density gradient electrophoresis and subsequently analyzed for their cell cycle phase. The following cultured cell types were investigated: human embryonic kidney cells at early passage, human T-1 aneuploid cell line, human NAM B-cell lymphoma, human MOLT-4 T-cell leukemia, mouse lymphoma L5178Y, Chinese hamster fibroblasts V79-171B, and Chinese hamster ovary CHO cells. Suspensions of cells were prepared in a Ficoll-sucrose buffer and subjected to upward vertical electrophoresis in a Ficoll-sucrose density gradient for 1.5 - 3.0 hr. The separated cells were collected in fractions and analyzed by flow cytometry after fixing and staining by the acriflavine-Feulgen method, which is stoichiometric for DNA/cell. In some cases cell fractions were re-cultured for subsequent growth-curve analysis. Both methods of analysis showed that the most rapidly migrating cells were mostly in G1 phase, and the slowest cells were predominantly in G2 phase at the time of electrophoretic separation. Migration velocity appears to decrease in a regular fashion from the beginning to the end of the cell cycle.

Work supported by research grant RO1 CA-24090 from the National Cancer Institute, National Institutes of Health, U.S. Public Health Service.

M-AM-Po130 A FAST, STABLE MICROELECTRODE VOLTAGE CLAMP. L. Ebihara* and R.T. Mathias. Department of Physiology, Rush Medical College, Chicago, Illinois 60612.

There are multiple problems to be overcome, if one is to attain a consistently fast and stable microelectrode voltage clamp. One problem is that the intracellular voltage recorded using a microelectrode is distorted or delayed by a time constant which is due to the high resistance and stray capacitance of the voltage recording electrode. We will present several interface designs which allow high fidelity wide band recording of membrane potential. Other problems stem from the large resistance R_I of the current passing electrode and the relatively small impedance Z_m of the preparation. Of these problems, the most difficult to solve is that the open loop gain of the voltage clamp is reduced by the ratio $Z_m(j\omega)/R_I$. At d.c. the reduction in gain may not be serious, but at high frequencies (or equivalently short times) the impedance of the preparation drops precipitously and this ratio becomes much more unfavorable. We will present general design criteria which render the stability and time response of the clamp independent (within reason) of this ratio. These criteria depend on the range of values one expects in the ratio $Z_m(j\omega)/R_I$. We have implemented a two microelectrode voltage clamp of clusters of embryonic chick heart cells grown in tissue culture. In this preparation we expect $Z_m(j\omega)/R_I$ to be no smaller than 10^{-4}, but stability and a 50 μ sec settling time are maintained in the presence of even smaller values of this ratio. Our explicit design will also be presented.

M-AM-Po131 METHODS FOR THE APPLICATION OF FLUORESCENT PROBES TO MICROSCOPIC ANALYSIS. S.C. Stringfellow, J.P. Leader*, J.J. Leader* and D.R. DiBona; Depts. of Physiology, Univ. of Alabama in Birmingham, Birmingham, AL 35294 and *Univ. of Otago, Dunedin, N.Z.

The incorporation of fluorescent probe technology to microscopic examination of transporting systems has been limited to a large extent by the inherent difficulty in quantifying the distribution of signal intensity among cellular components of interest. An effective solution is provided through the use of video digitization and computer handling of the retrieved images as arrays of 480 x 512 intensity values (picture elements or pixels) within 8-bit registers. Immediate advantages with this mode of data handling are: a) improvement of signal-to-noise ratio by signal averaging in each pixel; b) minimization of quenching with high-gain video cameras and very low levels of exciting illumination; c) serial analysis of induced or spontaneous changes in fluorescence within a small microscopic domain; and d) discrete analysis of multiple spectrally-distinct images. Demonstration of this methodology will be provided with examples from studies of the action of "potential-sensitive" carbocyanine dyes (DiOC[5],3 and merocyanine) and acridine orange (a weak base distributing with respect to pH gradients) on nucleated red blood cells and amphibian urinary bladder epithelium. Photodynamic damage which causes merocyanine redistribution in RBC's and the dissipation of mitochondrial membrane potential with valinomycin will be illustrated using false-color and intensity-distribution maps in time-lapsed studies. A number of possibilities for application of this technology to problems in epithelial transport will be discussed.

M-AM-Po132 DEVELOPMENT OF A CIRCULARLY VIBRATING MICROPROBE FOR MEASURING STEADY CURRENTS FROM LIVING TISSUE. J.A. Freeman and J.P. Wikswo, Jr., Dept. of Anatomy and Dept. of Physics and Astronomy, Vanderbilt University, Nashville, TN 37235

Little is known about the mechanisms that control the rate or direction of neurite growth. A host of studies suggest that many developmental and regenerative processes are regulated by intrinsic ionic currents. In order to investigate the inter-relationship between electric fields and growth cones of neurons growing in tissue culture, we have developed a miniaturized vibrating probe that is a significant improvement over that developed by Jaffe and Nuccitelli (J.Cell Biol., 1974). A platinized microelectrode is moved in a circle of 15-20 μm diameter at 500 Hz. The circular movement of the microelectrode is controlled by sine and cosine voltages, generated by a PDP 11/34 computer and applied to two miniature loudspeakers mounted at right angles. The microelectrode voltage V(θ), sensed by an ultra-low-noise amplifier, is averaged at each of 256 values of the angle θ around the circular path. The current density in the medium at the central point (x_o,y_o) can be shown to have components J_x and J_y given by the convolution integrals

$$J_x = -\frac{1}{\rho r}\int_o^{2\pi} V(\theta)\cos\theta d\theta \qquad J_y = -\frac{1}{\rho r}\int_o^{2\pi} V(\theta)\sin\theta d\theta$$

where ρ is the resistivity of the medium, and r is the radius of the circle. The computer evaluates these integrals for 1000 or more cycles of the probe to measure current densities as low as 5 nA/cm^2. Similar integrals can be used to determine the gradients of J at (x_o,y_o).

Supported by NIH Grant EY-01117-09 and an Alfred P. Sloan Research Fellowship.

M-AM-Po133 A LASER LIGHT SCATTERING PHOTOMETER FOR THE DETERMINATION OF MOLECULAR WEIGHT AND SHAPE OF BIOPOLYMERS. Dixie W. Frederiksen and Jerry P. Weir, Department of Biochemistry, Vanderbilt University, Nashville, TN 37232

The conventional Brice/Phoenix light scattering photometer was modified in several important ways. Most significantly, the mercury-xenon lamp was replaced by a 633 nm, linearly polarized, helium-neon laser. In addition, a photomultiplier tube, sensitive in the red range of the spectrum, has been used to detect the scattered light and to measure its intensity. The data is collected with a strip chart recorder. The resulting instrument provides an incident beam of far greater intensity than that of the original light source. Furthermore, the volume of the incident beam is reduced by more than an order of magnitude. As a result, the minimum sample volume necessary for experiments is reduced from about 25 ml to 3 ml, the minimum protein concentration required is reduced by a factor of two, and the procedures necessary for removal of dust and particulate material are greatly simplified. The accessible angular range is 20° to 135°. These changes are relatively inexpensive and greatly increase the usefulness of the instrument over that of the original photometer and over the commercially available low angle laser light scattering instruments as well. The modified instrument has been calibrated and used to verify the molecular weights of serum albumin and muscle actin. The polymerization of both brain and muscle actins has been followed with the light scattering apparatus.

(This work was supported by N.I.H. research grant NS-15077.)

M-AM-Po134 MASKED CONTRIBUTIONS TO THE CIRCULAR DICHROISM SPECTRUM OF SODIUM HYALURONATE.
M.K. Cowman, C.A. Bush, and E.A. Balazs*, Eye Research, Columbia University College of Physicians and Surgeons, New York, N.Y. 10032, and Department of Chemistry, Illinois Institute of Technology, Chicago, IL 60616.

The circular dichroism (CD) spectrum of sodium hyaluronate (NaHA; ($\xrightarrow{\beta\text{-}1,3}$GlcNAc$\xrightarrow{\beta\text{-}1,4}$GlcUA)) in H_2O was recorded to 180 nm using a computer-controlled vacuum ultraviolet CD instrument. The spectrum below 200 nm is complex, showing no clear bands attributable to the π-π^* transitions of the acetamido or carboxylate chromophores. In contrast, small oligosaccharides derived by enzymatic digestion of NaHA show CD spectra in H_2O with prominent bands centered near 190 nm. The oligosaccharide spectra can be matched as linear combinations of interior sugar residue (=NaHA) and end sugar residue CD contributions. End residues of the type GlcUA$\xrightarrow{\beta\text{-}1,3}$GlcNAc show a negative CD band near 190 nm. End residues of the type GlcNAc$\xrightarrow{\beta\text{-}1,4}$GlcUA show a positive CD band near 190 nm. Averaging of the two end residue spectra in the π-π^* region yields, perhaps fortuitously, an approximate match for the spectrum of NaHA. It is proposed that the complex spectrum of the polymer is the resultant of such oppositely signed contributions, which can be visualized by studying oligosaccharides. (Supported by NIH Grants EY 01747, EY 07002, AM 21826 and NSF Grant PCM 79-18887.)

M-AM-Po135 A MULTIPARAMETER FLOW-CYTOGRAPH.
Bo Thorell, Department of Pathology, Karolinska institutet, Stockholm, Sweden.

A cytofluorimeter capable of simultaneous 4-parameter analysis (i.e. endogenous fluorescence (NAD(P)H), exogenous fluorescent dyes, absorption and small angle scatter) is described. Analyses have been performed on isolated rat liver cells, white blood cells, bone marrow, thymus cells and yeast under different metabolic states. This allows correlations between cell function and concentration of cell substances, size, refractive indices, etc. Kinetic measurements are also possible, using time as additional parameter.

M-AM-Po136 QUANTITATIVE APPLICATION OF MULTIPLY-SCATTERED LIGHT TO NON-INVASIVE CLINICAL TESTING: Robert F. Bonner. Biomed. Eng. & Instr. Br., DRS, National Institutes of Health, Bethesda,MD., 20205

Most human tissues and fluids are characterised by a high number density of large (>λ) refractive index variations. Consequently, in situ optical measurements are confounded by a high degree of small angle multiple scattering.The application of proven single scattering techniques (e.g. LDV and angular scattering cross section) to human tissues and fluids have therefore been difficult. A theory has been developed to provide an excellent approximation of both coherent and incoherent multiple scattering effects. This theory approximates the dominant forward scattering by a radius dependent Gaussian form factor and multiple scattering as an anisotropic photon diffusion, which results in relatively simple analytic equations These equations have provided the basis for development and quantitative interpretation of a laser-Doppler tissue blood flow monitor and a simple low angle light scattering instrument to evaluate (without contamination) platelet viability of standard blood bank platelet concentrate units within their bags. The theory also allows the analysis of complex Doppler signals arising from contraction and blood flow in local regions of cardiac muscle in situ. Experimental data obtained in the above applications will be presented along with the theoretical formulations and interpretations.

M-AM-Po137 HIGH RESOLUTION NATURAL ABUNDANCE ^{13}C NMR SPECTRA OF INTACT MUSCLE. Donald D. Doyle and Michael Bárány, Dept. of Biol. Chem., Univ. of Illinois, Medical Center, Chicago, IL 60612.

Natural abundance proton-decoupled ^{13}C NMR spectra of intact frog, chicken, healthy and diseased human muscles were recorded at 90.5 MHz, 10-40°C. The observed resonances could be assigned to carbons located in phospholipids, proteins and soluble organic compounds in muscle (Doyle et al. FEBS Lett. 131, 147, 1981). The longitudinal relaxation time (T_1) of several resonances in intact muscle were compared with literature values of carbons in these compounds. The functional aspect of ^{13}C NMR was studied by comparing the spectra of caffeine-contracted frog gastrocnemius muscles with those of untreated contralateral resting muscles. A pronounced increase in the intensity of the 30 ppm (relative to TMS) resonance was found in the caffeine-treated muscle. Since the peak at 30 ppm is due to the $(CH_2)_n$ repeating unit of fatty acids in phospholipids, the increased intensity of the 30 ppm peak suggests increased motion of the aliphatic chains in muscle membranes as a result of caffeine action. In addition, the caffeine-treated muscles contained appreciable resonances for lactic acid at 21, 69.3 and 183 ppm which were virtually absent in the resting muscle. Apparently, the energy demand of caffeine contraction required the breakdown of some glycogen to lactic acid. This work represents the first approach for direct measurement of changes of lactic acid content during muscle contraction. (Supported in part by the University of Illinois NSF Regional Instrumentation Facility, grant NSF CHE79-16100, and by the Muscular Dystrophy Association. We thank David G. VanderVelde for his enthusiastic help).

M-AM-Po138 ^{13}C NMR STUDIES OF METABOLIC PATHWAYS IN VIVO. K.L. Behar, R.G. Shulman, J.R. Alger and J. Prichard. Department of Molecular Biophysics and Biochemistry and Dept. of Neurology, Yale University, New Haven, CT.

Recently we have been able to observe very well resolved ^{13}C NMR spectra from the acyltriglycerides in a human arm as well as in rats using an Oxford Research Systems TMR-32 spectrometer and a surface coil (1). In addition to these studies of the natural abundance ^{13}C peaks we have made measurements of the metabolism of ^{13}C labels introduced into a living rat as $1\text{-}^{13}C$ glucose. In one series of experiments the glucose was introduced into the rat through a stomach tube and the disappearance of the $[1\text{-}^{13}C]$ glucose peaks was followed in a TMR-32 NMR spectrometer over a period of several hours. Concurrently the appearance of a $[1\text{-}^{13}C]$ glycogen peak in the rat liver was monitored, and it was observed to reach a maximum intensity in ∿1 hour and to disappear in ∿14 hours. Rat brains which had been infused with $[1\text{-}^{13}C]$ glucose in the living animal were studied in a 10 mm sample tube in a 360 MHz NMR spectrometer after the animal was sacrificed. A relatively strong peak from $[3\text{-}^{13}C]$ lactate was observed when the animal had been made hypoxic but not when the animal had been sacrificed in a well oxygenated state. The signal-to-noise ratio of this peak was increased by the theoretical factor when a proton observe - ^{13}C decouple method of observation was used (2).

[1] Alger, J. et al. Science (in press).

[2] Sillerud, L.O., Alger, J.R. and Shulman, R.G. J. Magn. Res. (in press).

M-AM-Po139 ^{31}P NMR OF ARM AND BRAIN AS AN INDEX OF MITOCHONDRIAL PERFORMANCE. B. Chance, C. Barlow, L. Ligeti, L. Gulyi, S. Eleff, A. Sapega, D. Sokolow, Johns. Res. Fnd., U. of PA, Phila, PA. Spon. by: P. Mueller

Application of ^{31}P NMR to the exercising arm(1) and to the cat and gerbil stroke model(2) focuses attention upon the PCr/Pi ratios in the range 0.1 to ≈20.0 as characteristic of mitochondrial energy coupling in situ. Steady state arm exercise(1) drops PCr/Pi to the point of incipient lactic acidosis (PCr/Pi ∿ 1), and the minimum reached in an exercise bout to exhaustion is PCr/Pi ∿0.1. Recovery from such bouts of short-term hypoxia is uneventful and occurs in a $t_{\frac{1}{2}}$ of ∿5 min for normal and ∿7 min for patients with peripheral vascular disease. A similar stress is applied to the brains of animal models in transient hypoxia induced by breathing nitrogen; the recovery is rapid and uneventful, with a $t_{\frac{1}{2}}$ of ∿9 min after reestablishing tissue oxygenation. In prolonged incomplete ischemia such as obtained by bilateral carotid occlusion plus hypovolemia to MABP = 50, the time for recovery following reflow is ∿60 min following a 30min interval at PCr/Pi ∿o.1, tripling the interval of depleted energy state for the cortical tissue. The dissociation of energy coupling from electron transport is observed in this interval; optical observations indicate rapid reestablishment of electron transport in mitochodnria following reflow. The ability of mitochondria to raise PCr/Pi from 0.1(the level achievable by anaerobic glycolysis)to ∿20 in recovery from anoxic/ischemic results is a range in which mitochondrial energy coupling capabilities can be noninvasively and continuously monitored in the body tissues in normal and pathological states. (1)B.Chance et al., Proc.Nat'l.Acad.Sci.(USA),Nov 1981 in press.(2)B.Chance, in Transactions of the American Philosophical Society, in press. This research was supported by NIH grants GM27308, NS10939,HL18708.

M-AM-Po140 DIRECT ASSIGNMENT OF ISOLEUCINE TRANSFER RNA IMINO PROTONS BY NUCLEAR OVERHAUSER EFFECT.
Dennis R. Hare, Chemistry Department, University of Washington, Seattle, WA 98195

The most informative region of the ^1H NMR spectrum of tRNA is the extreme low field spectral region between 15 and 10 ppm, which contains a single exchangeable proton from each complementary base pair (the hydrogen bonded ring NH). Assigning each of the 27-28 low field protons to its corresponding base pair is not trivial and has been the subject of much controversy.

The spatial proximity of protons can be monitored via the NOE but its r^{-6} distance dependence reduces the NOE to only a few percent for interproton distances of ca. 4 Å. Nevertheless I have been able to detect the small NOE between the ring NH of a base pair and the ring NH of its nearest neighbor. Starting at base pair 14 a NOE was observed to the CG13 ring NH. By irradiating CG13 the base pair 12 resonance was found and base pairs 11 and 10 were similarly assigned leading to the assignment of all the D helix resonances.

In GU base pairs two ring NHs are within 2.8 Å and these two resonances are easily assigned by their large (30-50%) mutual NOEs. E.coli isoleucine tRNA contains GU pairs at positions 5 and 49. Starting at GU5 the resonances from base pairs 1,2,3,4 and 6,7 were assigned by NOE connectivity. By irradiating GΨ49 NOE assignments were made for base pairs 50,51,52,53,54,55. The helix 1-7 and the helix 49-55 were shown to co-stack in solution by 7-49 and 49-7 NOEs, thus assigning the top arm 1,2,3,4,5,6,7,49,50,51,52,53,54,55 of the L-shaped tRNA. Unambiguous assignments have now been made for all ring NHs by dipolar coupling - some of these direct assignments differ markedly from previous indirect assignments. (Supporting Grants GM28764 (NIH) & PCM8140603 (NSF)).

M-AM-Po141 PHOTOELECTRON MICROSCOPY OF MEMBRANE SOLUBLE CARCINOGENS AND DNA, William A. Houle, Dept. of Chemistry, University of Oregon, Eugene, Oregon, 97403.

Two major classes of chemical carcinogens are polycyclic aromatic hydrocarbons and aromatic amines. These lipid soluble compounds are taken up in cell membranes and metabolized to their ultimate carcinogenic forms by a series of membrane bound enzymes. To induce carcinogenesis the metabolically activated forms most likely bind to DNA. At present there is no general microscopic technique to determine the distribution of chemical carcinogens in cell membranes. A possible solution to this problem is to take advantage of an unexploited property of these molecules, the photoelectric effect. Upon absorption of light of sufficient energy molecules will emit electrons. Recent work has indicated that the photoelectron quantum yields (electrons per incident photon) of chemical carcinogens are several orders of magnitude greater than typical components of cell membranes in the wavelength range 180 to 250 nm [1,2]. Large differences in photoelectron quantum yield can be employed as a source of contrast in the photoelectron microscope where the emitted electrons are imaged. Calculations of relative contrast factors, electron statistics and beam current measurements indicate the feasibility of detecting small clusters or single molecules of carcinogen in biological membranes. Photoelectron micrographs showing the high contrast of carcinogens on biological substances have been obtained [1,2] and preliminary experiments suggest that it will be possible to image unstained DNA by photoelectron microscopy.

1. Houle, W.A., H.M. Brown and O.H. Griffith, Proc. Natl. Acad. Sci. U.S.A. 76 4180-4184 (1979).
2. Houle, W.A. and O.H. Griffith, Beitr. elektronenmikroscop. Direktab. Oberfl. 12 191-198 (1979).

M-AM-Po142 TECHNIQUE FOR INFERRING CAPACITANCE OF ARTIFICIAL LIPID BILAYER FROM CURRENT FLUCTUATION NOISE SPECTRA G. A. Nelson, Dept. Biophysics, SUNYAB 118 Cary, Main St. Campus, Buffalo, NY 14214

The aim of this technique is to determine the capacitance of a planar lipid bilayer while avoiding the disadvantages of other techniques. The technique of measuring charge or discharge time of a membrane with an electrometer is slow and has limited accuracy. An alternative technique which compares the voltage drop between a reference capacitor and the membrane capacitance provides an instantaneous readout of the membrane capacitance, but with the penalty of limiting the bandwidth to less than the test signal frequency. A new technique provides an instantaneous measure of the capacitance without perturbing the system with a test signal. The essential element is a voltage clamp of new design which provides a wide bandwidth output while preventing many extraneous contaminations of the output signal. Measurements with an audio spectrum analyzer or a Nicolet MED-80 show that the membrane capacitance is related to the maximum amplitude noise peak by the relationship $f_{max} \propto C_{mem}^{-1/2}$. The membrane capacitance determines the bandwidth of the system. This technique is useful for studying rapid membrane fluctuations such as noise in channels produced by antigen, antibody, and complement, or the noise from α-particle interaction with the bilayer.

M-AM-Po143 SPONTANEOUS CHEMILUMINESCENCE OF HUMAN BREATH-CORRELATION OF LUMINESCENCE INTENSITY AND HYDROGEN PEROXIDE CONTENT. M.D. Williams, D.A. Rodriquez, J.S. Leigh Jr. and B. Chance, Johnson Research Foundation, University of Pennsylvania, Philadelphia, PA 19104

The spontaneous chemiluminescence of human breath is quenched 50 to 90% by ingestion of 12 oz 5% alcohol and enhanced orders of magnitude by breathing pure oxygen. These observations coincide with the known quenching of free radical mediated luminescence and with the presently accepted theory of free radical mediated hypoxic stress. Chemical evidence for hydroperoxy type radicals in human breath is obtained by scopoletin fluorescence intensity decrease on reaction of hydrogen peroxide and horseradish peroxidase or by the cytochrome c peroxidase (CCP)-cytochrome c linked double beam spectrophotometric assay. The scopoletin assay indicates gradually lower hydrogen peroxide concentrations in the range of 10^{-6} moles hydrogen peroxide per liter of breath. The simultaneous measurement, with CCP, of hydrogen peroxide and luminescence intensity indicates a direct proportion between these variables for the first 100 breaths, against backpressure, measured. Luminescence intensity then increases despite a decrease in hydrogen peroxide concentration. This indicates the presence of luminescence not mediated by hydrogen peroxide in addition to luminescence that is mediated by hydrogen peroxide. Blocking the ultraviolet portion of the spectrum with a Wratten filter or lucite decreases the signal by approximately 30%. This indicates the presence of an emitter of near ultraviolet radiation in human breath, possible CO_2.

Supported by HL(SCOR) 15061.

M-AM-Po144 LIMITED PROTEOLYSIS OF TRANSDUCIN BY TRYPSIN. Cheryl Nash and Bernard Kwok-Keung Fung. Dept. Radiation Biology and Biophysics, University of Rochester Medical Center, Rochester, NY 14642.

The first stage of amplification in cGMP cascade in bovine retinal rod is carried out by transducin, a guanosine nucleotide binding protein consisting of two functional subunits: Tα (Mr ↶ 37,000) and Tβγ (Mr ↶ 35,000 and ↶ 10,000). Limited tryptic digestion of the purified Tα subunit initially removed a small segment from the polypeptide terminus and resulted in the formation of a single 36,000-dalton fragment. When this fragment was recombined with the intact Tβγ subunit, the reconstituted transducin exhibited greatly reduced GTPase activity and Gpp(NH)p binding capacity in the presence of photolyzed rhodopsin in membrane. The loss in activities was due to its inability to bind to the photolyzed rhodopsin. Prolonged digestion converted the 36,000-dalton fragment to a 32,000-dalton fragment that contained the guanosine nucleotide binding site. This 32,000-dalton fragment was resistant to cleavage in the presence of bound Gpp(NH)p, but was converted to two stable 23,000-dalton and 12,000-dalton fragments in the presence of GDP. Tryptic digestion of the Tβγ subunit resulted in two stable fragments (Mr ↶ 26,000 and ↶ 14,000 daltons) which, when recombined with the intact Tα subunit, exhibited 90% of the GTPase activity and Gpp(NH)p binding capacity. The results indicate that the guanosine nucleotide and rhodopsin binding sites are located in topologically distinct regions of the transducin molecule and raise the possibility that a large conformational transition of the molecule occurs upon the conversion of the bound GDP to GTP. (Supported by a grant from the National Eye Institute EY-03566.)

M-AM-Po145 LIGHT RELEASE OF Ca^{++} BY BOVINE ROD OUTER SEGMENT FRAGMENTS. Thomas G. Ebrey and Chang K. Suh, Department of Physiology and Biophysics, University of Illinois at Urbana-Champaign, Urbana, IL 61801

Ca^{++} selective electrodes, made with the neutral ligand ETH 1001, were used to measure light induced increases in Ca^{++} activity of suspensions of bovine rod outer segment fragments. In the presence of GTP, light can release significant amoungs of Ca^{++}. Bleaching 1% of a suspension containing $2.5 \cdot 10^{-9}$ moles of rhodopsin releases approximately $1.5 \cdot 10^{-9}$ moles of calcium. Omission of the GTP results in much smaller amounts of Ca^{++} released. Washing the rod fragments with Mg^{++} free buffer abolishes the ability of the fragments to release Ca^{++}; such a treatment is known to remove a GTP binding protein from the fragments (Hurley, Barry, and Ebrey, Biochem. Biophys. Acta 675: 359). We hypothesize that each light activated rhodopsin interacts with and releases Ca^{++} from many copies of a binding protein (perhaps identical with the GTP binding protein) in the rod outer segment fragments.

M-AM-Po146 EFFECT OF THE REMOVAL OF THE C-TERMINAL REGION OF BACTERIORHODOPSIN ON ITS LIGHT-INDUCED H^+ RELEASE AND UPTAKE. R. Govindjee, K. Ohno, and T. G. Ebrey, Department of Physiology and Biophysics, University of Illinois at Urbana-Champaign, Urbana, IL 61801

Removal of several residues from the C-terminal region of bacteriorhodopsin by digestion with trypsin or papain reduces the yield of light induced H^+ release by 50%-70%. The rate of H^+ release is not affected significantly, but the half-time of H^+ uptake increases almost two-fold. However, there is no effect on the photocycle of bacteriorhodopsin as judged by the yield and decay kinetics of the M412 photointermediate. H^+/M ratio in enzyme digested membranes is ~ 0.4 to ~ 0.8 whereas untreated membranes have a H^+/M ratio of ~ 2. Purple membrane sheets stored in distilled water at 4°C for prolonged period also have low H^+/M ratio, probably due to protease activity associated with bacterial contamination. Removal of the last four residues from the C-terminal end by carboxypeptidase A[1] does not affect the H^+/M ratio. Electrophoresis on SDS/polyacrylamide gels shows that both the enzyme treated and the stored purple membrane samples have a higher mobility compared to the fresh preparation and carboxypeptidase A treated membrane. The reduction in molecular weight can be accounted for by the loss of several residues from the C-terminal portion of the bacteriorhodopsin. We propose that the C-terminal region is partially responsible for the high yield of H^+ release from the purple membrane.

1. Gerber, G. E., C. P. Gray, D. Wildenauer, and H. G. Khorana. Proc. Natl. Acad. Sci. USA (1977) 74:5426-5430.

M-AM-Po147 INTRACELLULAR FREE Ca CONCENTRATION IS NOT A DIRECT INDICATOR OF THE RECEPTOR SENSITIVITY IN LIMULUS VENTRAL EYE. S. Levy, Boston University Medical Center and Marine Biological Laboratory, Woods Hole, MA 02543 (Intr. by E.F. MacNichol, Jr.)

Injection of Ca ions was shown to desensitize Limulus ventral photoreceptors. Using photometric methods, it was indeed demonstrated that Ca_i rises following illumination. The aim of this study was to try to quantitatively correlate levels of sensitivity and Ca_i using Ca selective microelectrodes based on neutral ligand. In the dark, the concentration of intracellular free Ca (Ca_i) was 0.27 ± 0.44 μM SD (n=7). During prolonged bright illumination, Ca_i transiently increased to 5.09 ± 4.29 μM SD, then gradually decreased to a value close to the dark level. The amplitude of the transient was graded with light intensity. In some cells, sensitivity was continuously monitored before and after penetration of the Ca selective microelectrode. Upon penetration by the Ca microelectrode, the cell sometimes lost as much as 3 log units in sensitivity, nevertheless Ca_i was still about 0.1 μm. In those cells, a bright prolonged stimulus caused Ca_i to transiently increase and then decrease to a value below the dark level. Both the transient increase and the undershoot were graded with light, the brightest stimuli inducing the largest transients and also the largest undershoots. On termination of the illumination, Ca_i gradually increased back to the dark level, with a time-course similar to the recovery of sensitivity. The findings that 1) a prolonged bright stimulus, leading to a sustained loss of sensitivity is not associated with a sustained increase in Ca_i, and 2) that a loss of sensitivity of a photoreceptor caused by penetration of a microelectrode is not associated with an increase of resting Ca_i are evidences that changes of sensitivity are not directly due to sustained changes in Ca_i.

M-AM-Po148 LIGHT INDUCED PROTON AND ION UPTAKE AND RELEASE BY BACTERIORHODOPSIN. T. Marinetti and David Mauzerall, The Rockefeller University, 1230 York Avenue, New York NY 10021

Transient changes in ionic conductivity on dye laser excitation (590 nm, 1 μs) in the linear energy response range of bacteriorhodopsin were monitored by phase sensitive detection of the signal from a symmetrical 100 kHz AC bridge sensitive to 1 ppm changes in conductivity. The heating of the solution remaining after completion of the ion pumping cycle serves as an internal calibration of the absorbed photons. The ratio of transient to thermal changes of conductivity gives directly the absolute quantum yield of ion release/uptake. The change of sign of the transient conductivity with differently charged buffers allows the absolute identification of the component of the transient which is due to protons, and whether ions are moving on or off the purple membranes. In acidic solution (pH 4 to 5) proton uptake occurs first (≈1 ms), followed by release (5 to 10 ms). This process is almost exclusively protonic and the quantum yield for it is roughly 0.3. In alkaline solutions (pH 8 to 10) a much larger conductivity increase is observed with ion release first (≈2 ms) and uptake later (≈10 to 100 ms) with only a small proton component. The quantum yield for this ion release is 2 to 3. Thus other ions besides protons are involved in the photoreactions of bacteriorhodopsin.

We thank Prof. W. Stoeckenius for gifts of bacteriorhodopsin and acknowledge the aid of NIH grant GM25693.

M-AM-Po149 EFFECTS OF LIPID ENVIRONMENT ON THE DECAY OF META I INTERMEDIATE OF RHODOPSIN. Patricia A. Baldwin and Wayne L. Hubbell, Department of Chemistry, University of California, Berkeley, CA 94720.

It has been previously reported that purified rhodopsin which has been incorporated into phospholipid bilayers containing only saturated phosphatidylcholine has a retarded rate of decay from metarhodopsin$_{478}$I, both above and below the lipid phase transition. A concurrent rise at 380 nm was observed, suggesting the appearance of the next normal intermediate, metarhodopsin$_{380}$II [O'Brien et al., Biochemistry 16:1295 (1977)]. We have investigated this phenomenon in greater detail and have found that recombinant membranes prepared from dimyristoylphosphatidylcholine or dipalmitoylphosphatidylcholine do not undergo the transition from meta I to meta II. Instead, in these systems, the 380 nm absorbing product of the slow meta I decay is retinal. Consistent with the fact that meta II is not produced, the usual proton uptake is not observed during the decay of meta I. Decay of meta I to retinal has previously been observed only in cases where rhodopsin is highly aggregated, such as lipid- and detergent-free rhodopsin or rod outer segment membranes in which 90% of the phospholipids have been hydrolyzed by phospholipase C treatment [Van Breugel et al., Biochim. Biophys. Acta 509:136 (1978)]. However, freeze-fracture electron microscopy and spin-labeling studies indicate that, in this case, the decay of meta I to retinal is not a result of rhodopsin aggregation, but rather is a direct effect of the interaction of rhodopsin with the lipid bilayer. Possible explanations of this effect will be discussed.

This research is supported by NIH grant #EY 00729.

M-AM-Po150 The Photoresponse of a Bilayer Lipid Membrane Containing Rhodopsin, Q.Y.Liu and H. Ti Tien, Department of Biophysics, Michigan State University, East Lansing, MI 48824

The fast photoresponse was observed from the bilayer lipid membrane (BLM) containing rhodopsin. The BLM was formed on a hole in a teflon cell. The forming solution consisted of a mixture of phospholipids in octane. Both compartments of the cell were filled with Ringer solution + 10 mM Tris-HCl at pH 7.0. One compartment also contained rod outer segment vesicles (prepared by ultrasonic treatment of a suspension of ROS which was isolated from dark adapted bovine retina). The observed potential elicited by an intense flash is very similar to the early receptor potential (ERP) from the eye or intact retina. The action spectrum of the photopotential matches the absorption spectrum of rhodopsin. The amplitude of the signal is proportional to the intensity of light when the intensity is not too strong ($<20 mW/cm^2$). The potential decreases with subsequent flashes. The potential increases with increasing concentration of rhodopsin in the bathing solution up to 10^{-5} M. The results suggest that the photoresponse is due to the conformational change of the rhodopsin molecules bound to the membrane or incorporated into the membrane. The photovoltage is not sensitive to pH change from pH 5.0 to pH 7.4. However, when the pH of the bathing solution is below 3, Components R_1 and R_2 of the ERP will, respectively, decrease and increase rapidly with decreasing pH. The R_2 rise and decay constants are similar to the results of the intact retina. The Arrhenius plot of R_2 rise constant is much higher than the Arrhenius plot of the reciprocal of the reaction time of Metarhodopsin II formation so R_2 can not be considered as directly representing Meta II formation. [Supported by NIH grant GM-14971]

M-AM-Po151 STABILISATION OF METARHODOPSIN I AT ROOM TEMPERATURE. Michel Tessier, Roger M. Leblanc and François Boucher, Centre de recherche en photobiophysique, Université du Québec à Trois-Rivières, Québec, Canada G9A 5H7.

Upon illumination, vertebrate rhodopsin undergoes a sequence of reactions accompanied by important spectral changes. Among them, the transition from Metarhodopsin I (λmax:480 nm) to Metarhodopsin II (λmax:380 nm) might be of great importance since it is thought to be closely related to the triggering of the visual excitation signal. We investigated that transition in purified rod outer segments (ROS) and detergent solubilised rhodopsin. In most detergents, like in ROS, Meta I decays to Meta II at temperature higher than 250 K. When Rhodopsin is solubilised in Lauryl ester of sucrose, Meta I is stable at temperatures up to 300 K. Spin labelling and fluorescence polarisation measurements indicate that the rigidity of the lauryl sucrose micelle might be responsible for that behavior.

Supported by NSERC of Canada and The Canada Council.

M-AM-Po152 CROSS-LINKING OF RHODOPSIN IN FROG ROS DISC MEMBRANES. Nancy W. Downer, Department of Biochemistry, University of Arizona, Tucson, Arizona 85721.

The distribution of oligomers produced by glutaraldehyde cross-linking of rhodopsin in isolated disc membranes was analyzed (by SDS gel electrophoresis) and compared to model predictions for intramolecular cross-linking of stable planar oligomers vs. cross-linking of diffusing monomers during random collisions. Results obtained on disc membranes were identical to those obtained by glutaraldehyde cross-linking of freshly dissected, dark-adapted frog retinas, but studies on disc membranes extended the range of cross-linking that could be observed and allowed measurement of the kinetics and extent of rhodopsin modification. These studies strongly support the conclusion that rhodopsin is a monomer in dark-adapted photoreceptors. The most important observations are 1) the observed distribution of oligomers is that predicted by random cross-linking in the range where the reaction is zero order. 2) ~40% of rhodopsin remains monomeric when reaction of lysine residues with glutaraldehyde has apparently saturated. Cross-linking of oligomeric enzymes under similar reaction conditions (0.1 mM glutaraldehyde, 0-10 hours) depletes monomer more rapidly and to a greater extent. 3) Cross-linking of opsin-containing disc membranes under the same conditions used to study dark-adapted samples frequently gave rise to a distribution of oligomers consistent with preferential (intramolecular) cross-linking where the predominant species is a trimer. Both the rate and extent of the cross-linking reaction was greater than for dark-adapted disc membranes. 4) Under the conditions used to analyze glutaraldehyde cross-linking in these experiments, $\geq$ 93% of rhodopsin migrated as the monomer in unreacted controls. (This work was supported by NIH Grant EY-03105).

M-AM-Po153 LIGHT AFFECTS RHODOPSIN-RHODOPSIN INTERACTIONS IN RECONSTITUTED PHOSPHOLIPID VESICLES: A FLUORESCENCE ENERGY TRANSFER STUDY. H. Borochov-Neori, P.A.G. Fortes and M. Montal, (Intr. by E.P. Geiduschek), Departments of Physics and Biology, UCSD, La Jolla, CA 92093.

We measured fluorescence energy transfer (FET) to monitor the proximity between purified rhodopsin (Rho) molecules labeled with either an energy donor or acceptor and reconstituted together in phospholipid vesicles. Sulfhydryl groups of Rho were labeled with either pyrenemaleimide (P-Rho) or monobromobimane (B-Rho), whereas ε-amino groups were conjugated with either dansylchloride (D-Rho) or FITC (F-Rho). The transfer efficiency (E) between P- and B-Rho was the same before and after bleaching. E was independent of the lipid to protein molar ratio (L/P) in the range of 50-400:1. It markedly decreased, however, upon the inclusion of unlabeled Rho (FET was no longer detectable when more than 60% of the protein was unlabeled), and was highly sensitive to the ratio of donor to acceptor (D/A). Vesicles containing D- and F-Rho exhibited FET only after bleaching. E was independent of L/P in the range of 100-400:1, but was highly sensitive to D/A. The results suggest that Rho was aggregated in the dark. After bleaching, the proximity between discrete regions of Rho monomers increased either within the pre-existing aggregate or due to a higher aggregation number. In D- and F-Rho, FET measurements placed the fluorophores approximately 35 and 40Å, respectively, from the endogenous chromophore, which seems to be located near the bilayer center[1]. Our studies, thus, detected light induced conformational changes in regions of Rho which are close to the membrane surface. These changes influenced Rho-Rho interactions, and may modulate the interactions of Rho with the peripheral enzymes as well. (Supported by Damon Runyon-Walter Winchell and NIH-EY02084, HE20262)

(1) Thomas, D.D. and Stryer, L. (1981) J. Mol. Biol. (in press).

M-AM-Po154 CRYSTALLINE MITOCHONDRIAL INCLUSIONS IN THE FROG ROD INNER SEGMENT. B.L. Scott. Dept. of Anatomy, Duke Univ. Medical Center, Durham, NC 27710.

The inner segment of frog retinal rod photoreceptors contains an area, called the ellipsoid, which is packed with mitochondria. The mitochondria are roughly 0.5μm in width and up to 6μm in length and are generally oriented parallel to the long axis of the photoreceptor. The present communication reports the observation of large crystalline inclusions within one of these mitochondria of the ellipsoid region.

Grassfrog retinas (Rana pipiens pipiens) were prepared for conventional electron microscopy: retinas were fixed with glutaraldehyde and osmium tetroxide, embedded in plastic, serially thin-sectioned and counterstained with uranyl acetate and lead citrate. Electron microscopic examination of the serial thin sections revealed a single, unusually large mitochondrion (1.8μm X 3.5μm in the plane of the section) which contained several crystalline inclusions.

The inclusions are long and narrow, measuring from 0.05 to 1.0μm in width and up to 3μm long. They are bounded by membrane and contain hexagonally packed circular densities 3 to 4 nm in diameter, with a center to center spacing of approximately 9 nm. Optical diffraction of micrographs of the inclusions shows six strong first order diffraction spots and six weak second order ones. The inclusions reside between the inner and outer mitochondrial membranes and perhaps within some cristae, suggesting the inclusions may be composed of a protein confined to the intermembrane space, such as adenylate kinase. E. Yamada observed similar inclusions in frog retinal rod inner segments (J.Biophys.Biochem.Cytol. 4:685 (1958)). The composition and cause of formation of the inclusions is unknown. Supp. by Duke Fellowship to BLS,& USPHS Grants EY-00016&EY-01659 to Dr. J.M. Corless.

M-AM-Po155 CHARACTERIZATION OF BOVINE ROD OUTER SEGMENT G-PROTEIN. Wolfgang Baehr, Elaine A. Morita, Richard J. Swanson, and Meredithe L. Applebury, Department of Biochemical Sciences, Princeton University, Princeton, New Jersey 08544.

Bovine ROS G-protein consisting of three subunits (α with 41K, β with 37K, and γ with <10K mobility) can be eluted from fully bleached membranes by ∿μM GTP in low ionic strength buffers. GTP or its non-hydrolyzable analogue GMPPNP elute G-protein equivalently indicating that GTP hydrolysis is not required for the release from the membrane surface. The binding constant for the GMPPNP*G-protein complex is $0.5 \times 10^7\ M^{-1}$ with 1 mole nucleotide bound per mole of G-protein (assuming MW 80,000). G-protein is inhomogeneous in solution and can be separated into two species by native gel electrophoresis. The faster moving one was identified as a dimer of G-α by second dimension gel electrophoresis and analytical ultracentrifugation, the slower moving one as a dimer of G-βγ which has a tendency to form tetramers or higher aggregates at moderate ionic strength. Peptide maps and isoelectric points indicate G-α and G-β are distinctly different polypeptides. G-α, G-βγ, and purified G-protein can be reconstituted with bleached depleted membranes. A GTP hydrolytic activity could be restored only in the presence of all three subunits. The turnover number of this GTPase is approximately 1.0 mole GTP/mole G-protein/min. Binding saturation of ROS membranes is reached at 1 mole G-protein to 4 moles of rhodopsin.

M-AM-Po156 CHAPS, A USEFUL NEW DETERGENT FOR THE STUDY OF VISUAL PIGMENTS. Allen Kropf and Stephen G. Milheim, Department of Chemistry, Amherst College, Amherst, MA 01002.

CHAPS, an acronym for 3-[(3-cholamidopropyl)dimethylammonio]-1-propanesulfonate, is a synthetic, zwitterionic derivative of cholic acid whose synthesis has been described by Hjelmeland (PNAS 77, 6368 (1980)). Measurement of the critical micelle concentration (cmc) by a differential refractive index method yielded a value of 3.9 ± 0.1 mM in 0.067 M PO_4 buffer, pH 6.5 at 23°C. Rhodopsin from purified cattle rod outer segments is readily solubilized in 6 mM CHAPS yielding 3-4M rhodopsin solutions which do not sediment when centrifuged at 100,000 g for short periods. Rhodopsin in CHAPS shows almost the same thermal stability as it does in 2% digitonin solution with $\Delta G^{\ddagger}$ = 23.5 Kcal/mole at 58°C in 9 mM CHAPS and $\Delta G^{\ddagger}$ = 23.3 Kcal/mole at 58°C in 2% digitonin, both at pH 6.5. Following photochemical bleaching of rhodopsin in CHAPS and in 2% digitonin, rhodopsin regenerated more rapidly and more completely in CHAPS. Though rhodopsin's absorption spectra in CHAPS and digitonin are identical as are their photosensitivities, their CD spectra differ. In CHAPS the α-band has its λ_{max} at 498 nm and the β-band is relatively smaller than in other detergents. Thus the hypsochromic shift of λ_{max} of the CD α-band, seen in all other detergents, is absent in CHAPS solubilized rhodopsin. (Supported by NIH Grant EY00201 and the NSF-URP program.)

M-AM-Po157 ORIGIN OF DELAYS IN PDE ACTIVATION OF ROD DISK MEMBRANES (RDM). P.A. Liebman, A. Sitaramayya and E.N. Pugh, Jr., Dept. of Anatomy, Univ. of Pennsylvania, Phila., PA 19104.

A 10^{-5} flash bleach ($h\nu$) conveys its full effect on PDE activation of RDM suspensions after a delay of 1-3 sec attributed to a rhodopsin (Rh) lateral diffusion-mediated serial activation multiplier[1,2] in RDM suspensions (GTP cofactor, no ATP). Pure PDE (P) and GTP-binding protein (Γ) added to RDM stripped of peripheral proteins (SRDM) at 100 Rh:20 Γ :2 P gives similar light sensitivity and delay. The delay is also seen for the addition sequence (SRDM·Γ·P + $h\nu$) + GTP or (SRDM·P + GTP + $h\nu$) + Γ but not for (SRDM·Γ + GTP + $h\nu$) + P. (SRDM·Γ +GTP + $h\nu$) + (RDM·P) gives normal activation while (SRDM·P + GTP + $h\nu$) + (RDM·Γ) activates poorly suggesting that Γ·GTP can leave the Rh* membrane to activate other P's while neither Γ·GDP nor P can transfer effectively. The absence of activation delay on final P addition together with failure of P to dissociate readily from RDM at normal ionic strength shows that P could not dissociate from dark RDM to become activated on bleached RDM in times less than $\sim 10^4$ sec. A similar constraint limits departure of Γ·GDP. Collision theory shows that Rh* and Γ·GDP could only undergo 1-10 collisions sec^{-1} at the diffusion limit if Γ·GDP "hopped" through the solution while our α ^{32}P-GTP labelling work[3] shows that Γ·GTP's are produced at $\sim 10^3 sec^{-1}$ by each Rh*, a rate easily accounted for by lateral diffusionally mediated collisions between Rh* and Γ·GDP bound to the same RDM. The binding constant for the RDM of the Γ*·GTP's produced is sufficiently low to allow Γ*·GTP escape from the originating RDM to the aqueous surroundings through which it does serve as a diffusible activator of P on non-bleached RDM. [1]Yee & Liebman (1978) J. Biol. Chem. 253:8902. [2]Liebman & Pugh (1979) Vis. Res. 19:375. [3]Liebman & Pugh, Biophys. Abstracts, 1980. Supported by EY00012 and EY01583.

M-AM-Po158 MECHANISM OF ATP-MEDIATED QUENCH OF PDE ACTIVATION IN ROS. A. Sitaramayya, P.A. Liebman and E.N. Pugh, Jr. Department of Anatomy, University of Pennsylvania, Phila., PA 19104.

ATP rapidly quenches weak light-activation of PDE in normal bovine rod disc membrane (RDM) preps. To learn what RDM proteins are responsible for this important controller effect, peripheral proteins from RDM [PDE, GTP binding protein (Γ), rhodopsin kinase and others] were removed, concentrated and added back to RDM stripped of these proteins to form recons. Some of the stripped RDM preps were thermolysin treated (TL+) to remove the C-terminal segment of rhodopsin, a 12-amino acid chain rich in serine and threonine known to be the site of rhodopsin kinase-mediated phosphorylation.[1] The effect of ATP on initial PDE velocity (V_o) and PDE turn-off time (τ_{off}) were compared for TL+ and normal(TL-)recons. We observed that 1) ATP reduced V_o in both TL+ and TL- recons; 2) ATP reduced τ_{off} of TL- recons but had no significant effect on τ_{off} of TL+ recons; 3) AMPPNP increased τ_{off} by about 20% in both TL+ and TL- recons. A further effect of thermolysin was to increase V_o for both strong and weak bleaches. These observations suggest that the C-terminal end of rhodopsin mediates ATP quenching of PDE activation, possibly through the action of rhodopsin kinase. Since AMPPNP can increase τ_{off} in the presence of GTP, both GTP and ATP must be able to serve the apparent τ_{off} phosphorylation mechanism, as previously noted by Liebman and Pugh.[2] Higher V_o of TL+ compared to TL- suggests the C-terminal segment of bleached rhodopsin may also partly occlude the Γ activator site of rhodopsin.[3] Supported by NIH grants EY00012 and EY01583.

[1] Hargrave et al. (1980) Neurochem. Int. 1: 231.
[2] Liebman and Pugh (1980) Nature 287: 734.
[3] Aton and Litman, ARVO Poster, 1980.